

AD-A038 528

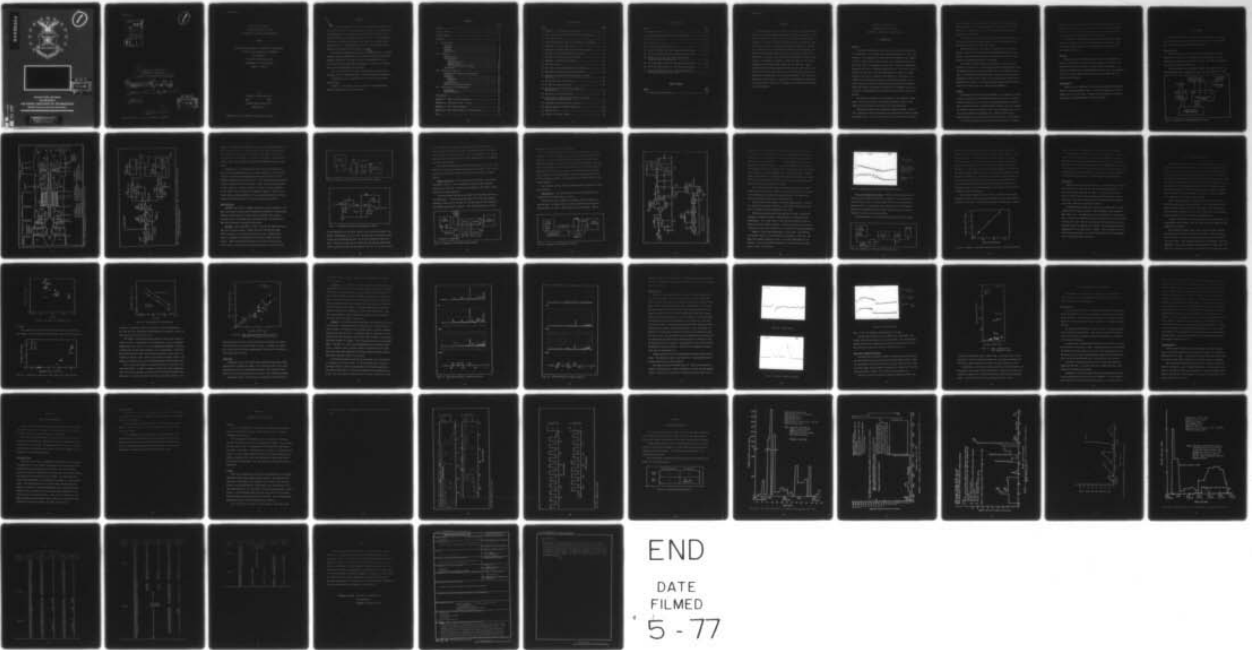
AIR FORCE INST OF TECH WRIGHT-PATTERSON AFB OHIO SCH--ETC F/G 14/2
A METHOD FOR ANALYSIS OF ELECTROSTATIC PROBE SIGNALS RELATING T--ETC(U)
DEC 76 W E GIFFORD

UNCLASSIFIED

AFIT/GNE/PH/76-3

NL

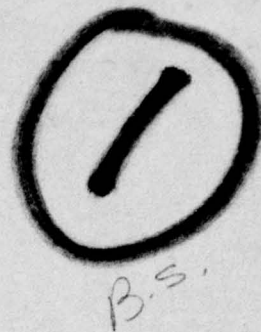
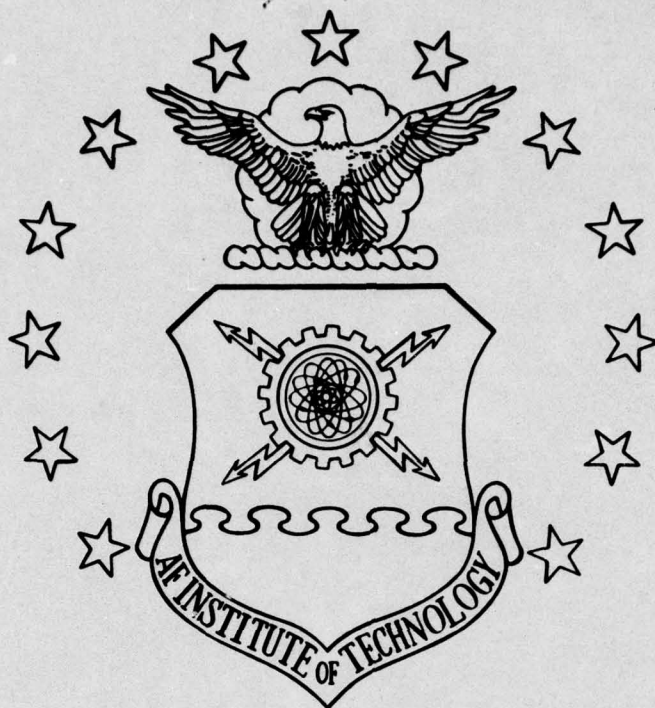
1 of 1
ADA038528



END

DATE
FILMED
5 - 77

ADA 038528



UNITED STATES AIR FORCE
AIR UNIVERSITY
AIR FORCE INSTITUTE OF TECHNOLOGY
Wright-Patterson Air Force Base, Ohio

AD NO. _____
DDC FILE COPY

DISTRIBUTION STATEMENT A

Approved for public release;
Distribution Unlimited



ACCESSION FOR	
WHS	White Section <input checked="" type="checkbox"/>
WSP	Buff Section <input type="checkbox"/>
UNANNOUNCED	<input type="checkbox"/>
IDENTIFICATION	
DISTRIBUTION/AVAILABILITY CODES	
Dist.	AVAIL. and/or SPECIAL
A	

6

A METHOD FOR ANALYSIS OF
ELECTROSTATIC PROBE SIGNALS
RELATING TO JET-ENGINE MICRODISTRESSES.

14

AFIT/GNE/PH/76-3

10

THESIS

Edward

William R. Gifford, III

Capt USAF

9

Master's thesis,

11

Dec 76

12

62p.

DDC

RECEIVED

APR 22 1977

RECEIVED

D

1473

012225

Approved for public release; distribution unlimited

GNE/PH/76-3

A METHOD FOR ANALYSIS OF
ELECTROSTATIC PROBE SIGNALS
RELATING TO JET-ENGINE MICRODISTRESSES

THESIS

Presented to the Faculty of the School of Engineering
of the Air Force Institute of Technology
Air University
in Partial Fulfillment of the
Requirements for the Degree of
Master of Science

by

William E. Gifford III, B.S.


Capt USAF

Graduate Nuclear Engineering

December 1976

Approved for public release; distribution unlimited.

Preface



This thesis is part of an ongoing effort to develop a system which can reliably predict jet-engine gas-path failures. If this system became operational it could result in a significant reduction in jet aircraft losses due to gas-path component failure. This study was the first effort to develop a system for analyzing tape recorded data of engine failures. A tape recorded failure had the advantage that an observer could replay the failure many times.

Two pieces of equipment greatly aided me in this study. The bolus counter circuit was designed by Mr. T. Molnar of the Air Force Flight Dynamics Laboratory. The delay circuit was designed and built by Mr. G. Gergal of the AFIT Physics department. I would like to thank both of these individuals for their help.

Mr. D. Myers and Mr. T. Larkin, both at Detroit Diesel Allison Division, were of considerable help in providing data for correlation.

I would also like to thank Major R. P. Couch for his help and encouragement.

Finally, I would like to thank my wife for her understanding, patience and help during my tour at AFIT.

Contents

	Page
Preface	ii
List of Figures	iv
List of Tables.	v
Abstract.	vi
I. Introduction.	1
Overview	1
Purpose.	2
Approach	3
Organization	3
II. Equipment	4
Data Recording	4
Data Reduction	9
Raw Data	9
Engine Vibrations.	11
Photoanalysis.	12
Pulse Area Integration System.	15
Limitations.	17
III. Experimental Results.	18
Probe Current Traces as an Indication of Stress.	20
Vibrations	23
Compressor	24
Turbine.	24
Photoanalysis.	27
Pulse Area Integration System.	29
IV. Conclusions and Recommendations	31
Conclusions.	31
Recommendations.	32
Bibliography.	34
Appendix A: Theory of Bolus Formation.	35
Appendix B: Profiles of A and C Cycles	37
Appendix C: TF-41 Failure History.	41
Appendix D: Bolus Count History for TF-41 S/N 908.	48
Vita.	52

List of Figures

<u>Figure</u>	<u>Page</u>
1 Schematic of Recording Equipment Setup.	4
2 TF-41 Tailpipe with Electrostatic Probes Installed.	5
3 Electrostatic Probe	6
4 TF-41 Cross-sectional View with Location of Vibrometers	7
5 Schematic of Bolus Counter Circuit.	8
6 Schematic of Current Level and Pulse Count System	10
7 Schematic of Bolus Box Preamplifier Circuit	10
8 Schematic of Vibration Analysis System.	11
9 Schematic of Photoanalysis System	12
10 Delay Box Circuit	13
11 Saturation Pulse Showing Effect of AC Coupling.	15
12 Schematic of Pulse Area Integration System.	15
13 Relation of Integrated Pulse Area Count to Actual Pulse Area.	16
14 LP2 Turbine Damage TF-41 S/N 908.	19
15 DC Level as a Function of T_1	21
16 DC Level as a Function of Gross Thrust for TF-41 S/N 908	21
17 Thrust vs T_1 for TF-41 S/N 908.	22
18 Pulse Count vs Average HPSS DC Level of 2:30 and 6:30 Probes in TF-41 S/N 908.	23
19 Compressor Vibration Frequency Spectrum	25
20 Turbine Vibration Frequency Spectrum.	26
21 Bipolar Pulse	28
22 Series of Monopolar Pulses.	28

List of Figures

<u>Figure</u>	<u>Page</u>
23 Saturation Pulse.	29
24 Pulse Integrated Area Count vs HPSS DC Level.	30
B-1 Profile of A Cycle.	39
B-2 Profile of C Cycle.	40
C-1 Failure Correlation Matrix.	41
C-2 TF-41 S/N 141050 (B.U. 16) Particle Count vs Time.	42
C-3 TF-41 S/N 141050 (B.U. 18) Particle Count vs Time.	43
C-4 Electrostatic Probe Test - Positive Particle Count vs Engine Running Hours	44
C-5 TF-41 S/N 141050 (B.U. 52) Particle Count vs Time.	45
C-6 TF-41 S/N 141050 (B.U. 17) Particle Count vs Time.	46
C-7 TF-41 S/N 141050 (B.U. 18) Peak Particle Count vs Time (First 308 Hrs. of B.U. 18).	47

List of Tables

<u>Table</u>	<u>Page</u>
I TF-41 S/N 908 Bolus Counts.	49

Abstract

Various methods of data reduction to correlate electrostatic probe signals with engine gas-path distress were developed and tested. These methods consisted of counting pulse signals, monitoring turbine and compressor vibrations, examining individual pulses to determine significant characteristics, and using the integrated areas of all pulses in a given test cycle to determine the level of engine distress. The systems developed were tested using tape recorded data from a TF-41 undergoing a simulated flight endurance test at Detroit Diesel Allison Division in Indianapolis, Indiana. During the test, the LP2 turbine experienced a non-catastrophic failure due to a seal rub. Tapes recorded during the test indicate that the failure occurred over an 80 hour period in which large (350 msec long, 8 volts high) pulses were observed on accelerations. The vibration signature of the engine also changed during this period. A system which integrated the areas under the pulses showed a factor of 20 increase during the period of highest recorded distress.

A METHOD FOR ANALYSIS OF
ELECTROSTATIC PROBE SIGNALS
RELATING TO JET-ENGINE MICRODISTRESSES

1. Introduction

Overview

A gas-path microdistress is defined as an event which takes place in the gas-path of a jet engine that places metal particles, ions, free electrons, or a combination of these into the flowstream. For example, a rubbing turbine blade or metal erosion in the combustor section of the engine would be a gas-path microdistress. It has been established experimentally, both in laboratory simulation (Ref 1,5,7) and in actual engine tests (Ref 3,8), that microdistresses form pockets of charge (boluses) which can be detected in the exhaust of a jet engine. The frequency of microdistress formation, and therefore boluses, can increase with time, signifying increasing engine component degradation. Thus, there exists the potential of detecting an impending engine failure before instrumentation such as RPM or EGT gauges would indicate a problem.

The method of formation of these boluses is not completely understood. This does not alter the documented evidence, however, that appearances of boluses are correlated with microdistresses.

A method for reducing and interpreting data was needed. Prior to 1976, signals from this electrostatic probe system had not been recorded on magnetic tape. Thus, only limited data on a given failure was avail-

able to observers. This data was in the form of oscilloscope photographs and number of pulses per unit time. The failure could not be replayed and correlated with other engine parameters such as inlet temperature or vibrations.

The purpose of this study, then, was to evaluate methods for reducing and interpreting signals caused by bolus interaction with an electrostatic probe in a jet-engine tailpipe.

During the period of this study, a gas-path failure did occur. Unusually large (320-380 msec long and 8 volts high) pulses were observed. This provided an excellent opportunity to evaluate the data reduction methodology proposed in this study.

This report will show that it was possible to detect an engine distress as it occurred. The distress was easily distinguishable above the background data by a factor ranging from 2 to 100 depending on the type of discriminating electronics used. The report will also show a relationship between the DC level of the exhaust and the gross thrust produced by the engine. This latter finding warrants further study by itself since gross thrust is a useful engine parameter.

Purpose

The purpose of this thesis is threefold: 1) to establish a means of quickly determining when tape-recorded data varies from an established background norm; 2) to test and recommend methods of reducing data to provide warning of severe gas-path distress; and 3) to attempt to correlate observed signals with other engine parameters for a TF-41 jet engine undergoing a simulated flight endurance (SFE) test at General Motors Corp., Detroit Diesel Allison Division in Indianapolis.

To determine whether the ion probe detection system is reliable

enough to be used as a standard engine failure warning device, a large number of engines must be tested. To minimize the costs for manpower and equipment, a method must be devised by which data can be quickly screened and insignificant data can be eliminated.

The SFE test at Allison Division was used to develop the methods necessary to accomplish the first two purposes. In addition, a non-catastrophic engine failure, which occurred during the test period, was examined in detail.

Approach

Signals from two ion probes, high speed and low speed spool RPM (N_H and N_L respectively), and turbine and compressor vibrations were recorded on an FM tape recorder by Allison Division personnel. The tapes were transferred to Wright-Patterson AFB where they were examined. The results of this study were used to establish a method for data reduction and analysis.

Organization

Chapter II is a discussion of the various equipment setups developed to record and reduce the data. Chapter III contains the experimental results of this study. Chapter IV gives conclusions based upon this study and recommendations for further studies.

II. Equipment

This chapter provides a description and discussion of the equipment setup used to record the data at Detroit Diesel Allison Division and to reduce the data at Wright-Patterson AFB.

Data Recording

The system shown in Fig. 1 was used to record data at Detroit Diesel Allison Division in Indianapolis. A TF-41 turbofan engine (S/N 908) was used as the source of the data. The TF-41 was undergoing a simulated flight endurance test.

The test consisted of a series of engine runs called "cycles" at three specified inlet temperatures (T_1): 70°, 90°, and 110°F. Three

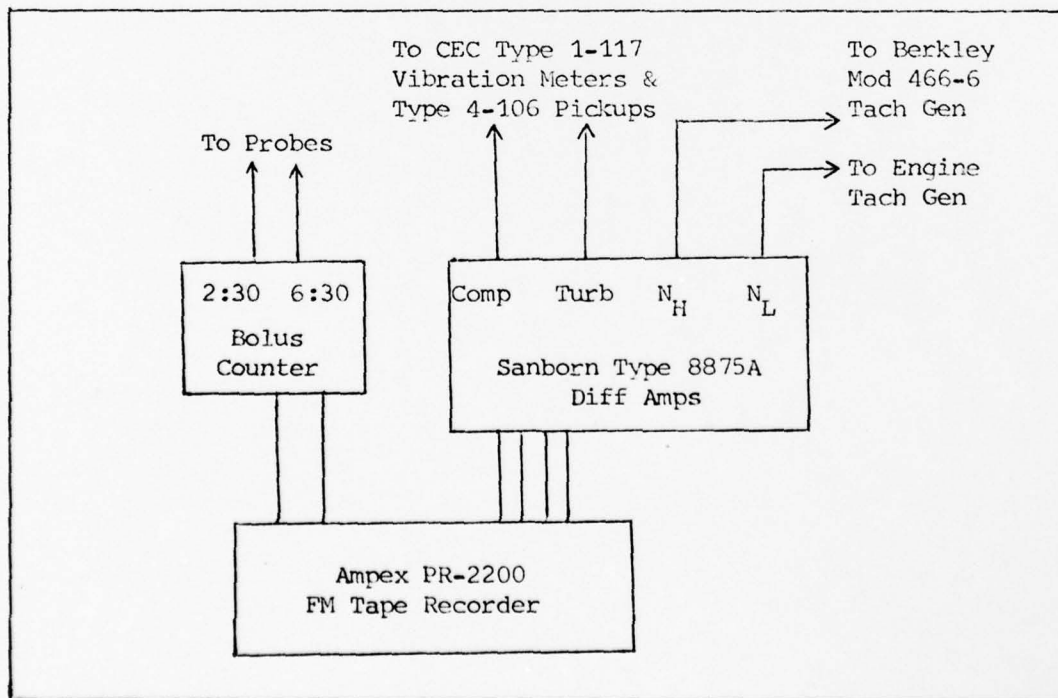


Fig. 1. Schematic of Recording Equipment Setup

types of cycles were run: A, B, and C. (See Appendix B for profiles of the A and C cycles.) Since an A cycle has the most severe stress profile, consisting of rapid accelerations and decelerations, it was decided that A cycles should be recorded continuously, along with a sampling of C cycles. The B cycles were not used in this study since the power settings reached by an engine during a B cycle were not high enough to produce boluses.

Two electrostatic probes were installed in the tailpipe of the engine in the 2:30 and 6:30 o'clock positions (Fig. 2). The probes were identical to that shown in Fig. 3.

Vibration data was monitored on the compressor and turbine sections of the engine. A CEC Type 1-117 Vibration Meter with a Type 4-106 pick-

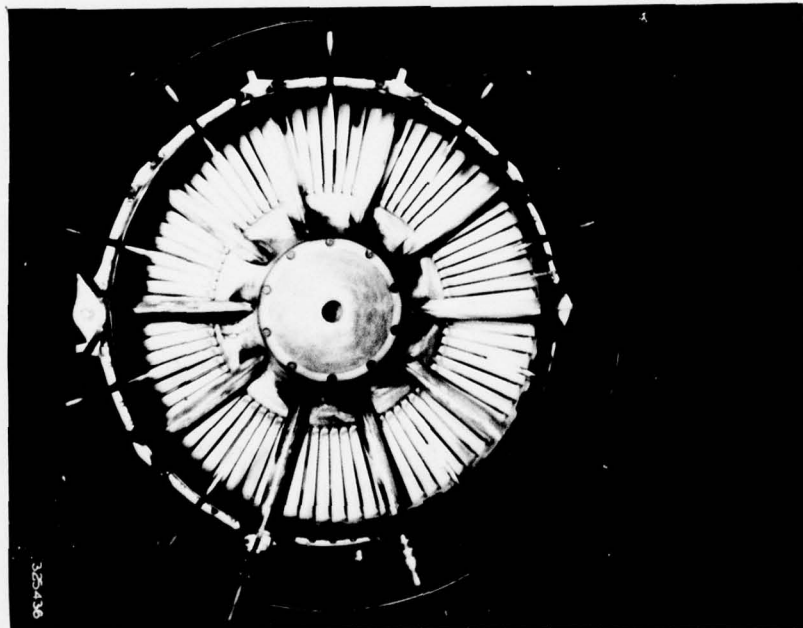


Fig. 2. TF-41 Tailpipe with Electrostatic Probes Installed.

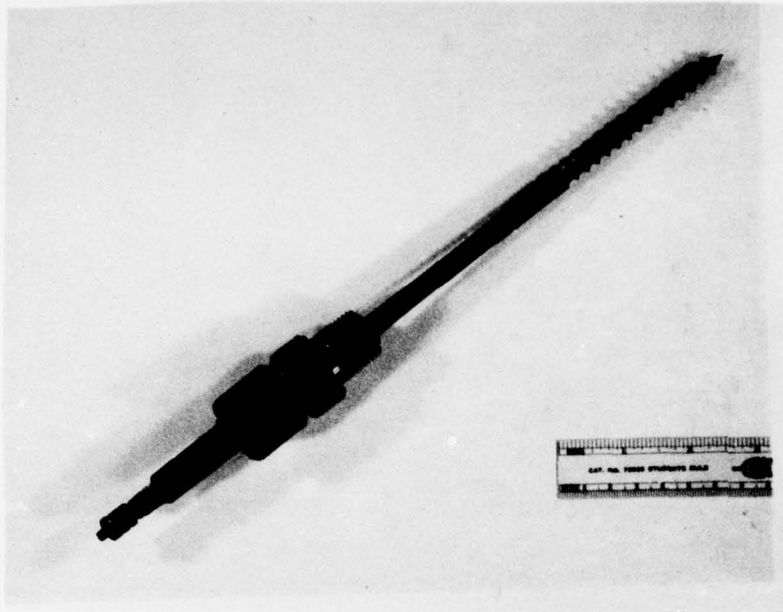


Fig. 3. Electrostatic Probe

up, located as shown in Fig. 4, was used on each section. The resultant signals were passed through Sanborn Type 8875A differential amplifiers to the tape recorder.

The high speed (N_H) and low speed (N_L) spool RPM's were also recorded. A Berkley Mod 466-6 Tach Generator produced the N_H RPM signal. The TF-41 Engine Tach Generator produced the N_L RPM signal. Both signals were passed through Sanborn Type 8875A differential amplifiers before being recorded.

The probe signals went to the Bolus Counter circuit shown in Fig. 5. The raw signal went to the tape recorder where it was reduced by a factor of 10 before being recorded. This was done to prevent saturation of the tape recorder by the pulses which regularly had an amplitude of 8 volts.

The raw signal also went to a logic circuit which triggered a 2 volt square wave whenever a ± 2 volt threshold was exceeded. If the

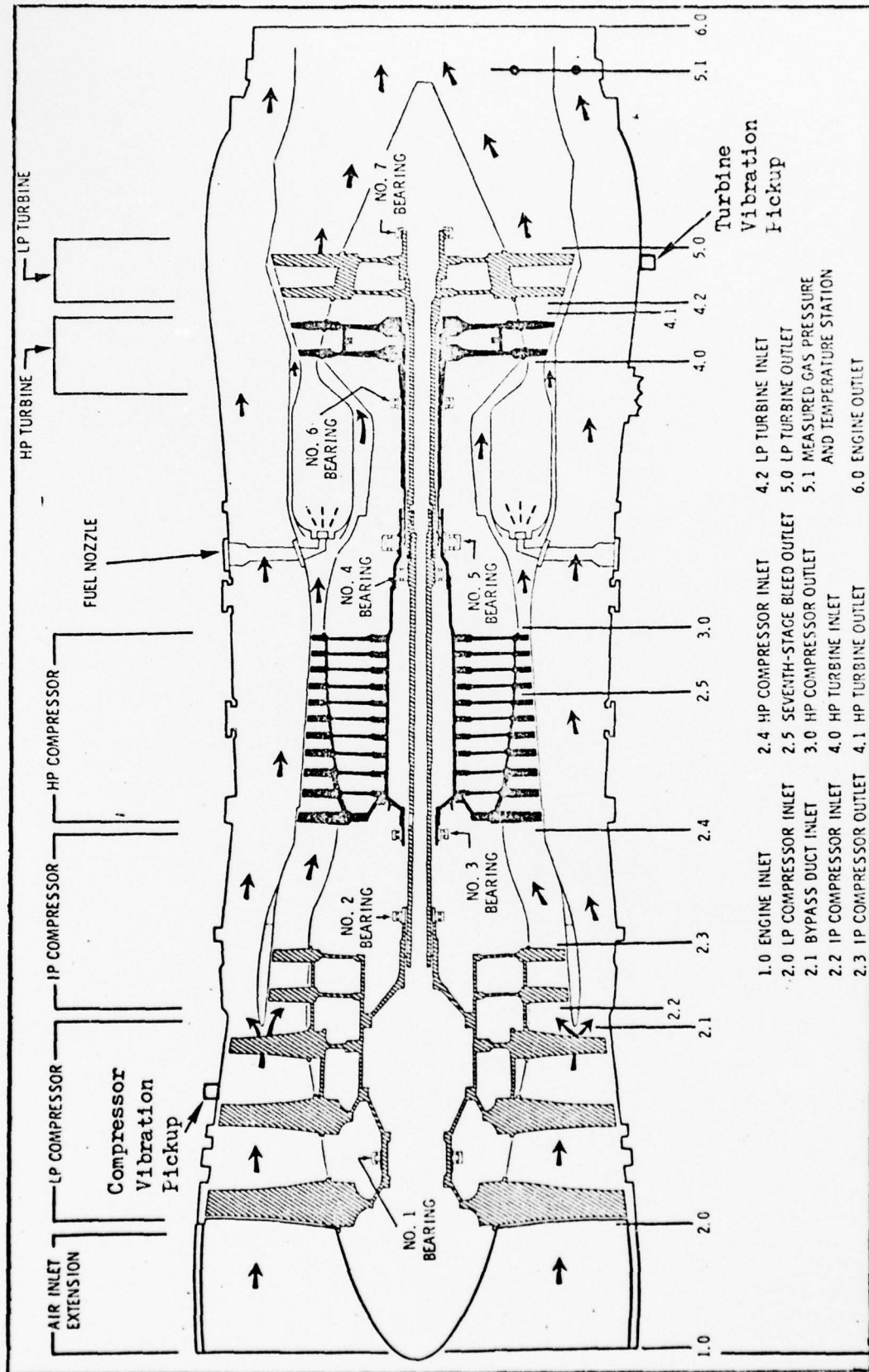


Fig. 4. TF-41 Cross-sectional View with Location of Vibrometers

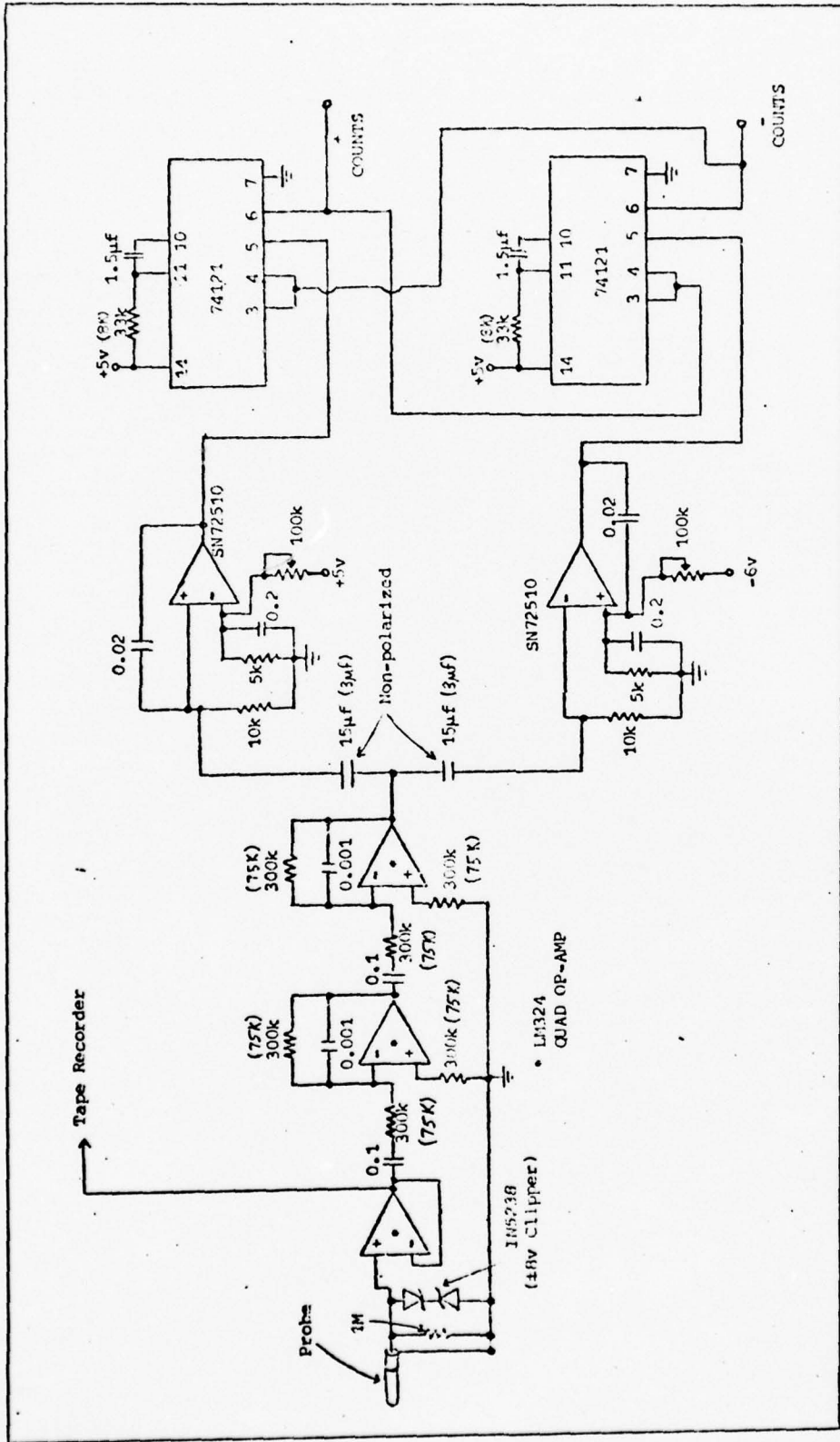


Fig. 5. Schematic of Bolus Counter Circuit. Note: The values in parentheses refer to the circuit used at WPAFB.

positive threshold was exceeded, the square wave was generated by the positive count circuit. If the negative threshold was exceeded, the square wave was generated by the negative count circuit. The RC time constant was set at 35 msec. The output of the logic circuit went to a counter system which totaled the positive and negative counts for each probe.

Unexpectedly, this system made a nearly ideal discriminator for the large pulses associated with the observed failure. Prior to this failure, the widest pulse observed had been about 20 msec long (Ref Private communication with Major Couch). This was the basis for setting a 35 msec "dead time" for the circuit. When a positive pulse exceeded 35 msec, however, it caused a count (or a number of counts depending on its actual width) to occur in the negative channel. There were few actual negative pockets observed. Thus, the negative channel served as a pulse width discriminator for pulses more than 35 msec wide.

Data Reduction

Equipment was set up to examine four basic areas of interest: raw data from current traces, engine vibrations, photoanalysis of individual pulses, and determination of pulse sizes (integrated pulse areas). Although some of the systems were used concurrently, the setups have been drawn separately to simplify discussion.

Raw Data. The system shown in Fig. 6 was used to examine the raw data of the current traces. Signals from the 2:30 and 6:30 probe tracks were sent to the bolus box where two 10 to 1 preamplifiers, (Fig. 7), restored the amplitudes of the traces to their original values. These signals then proceeded to the logic circuits of the bolus counter circuit where they produced signals in a manner similar

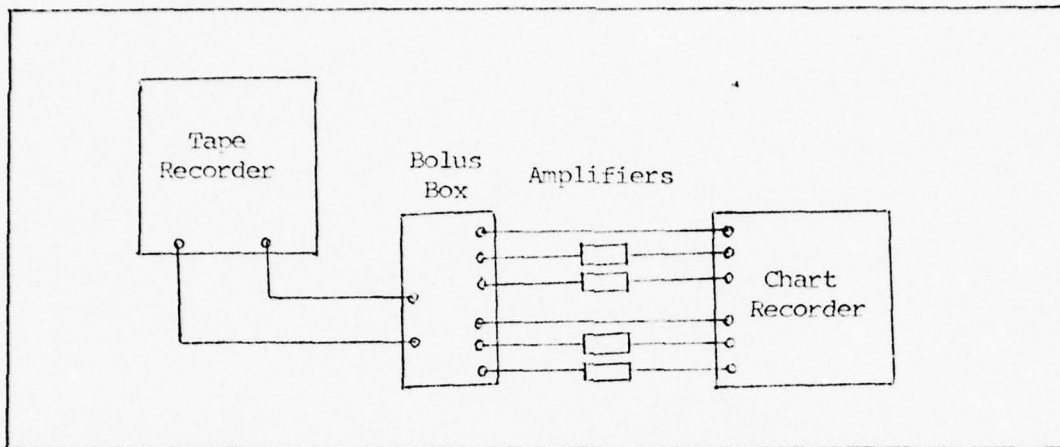


Fig. 6. Schematic of Current Level and Pulse Count System

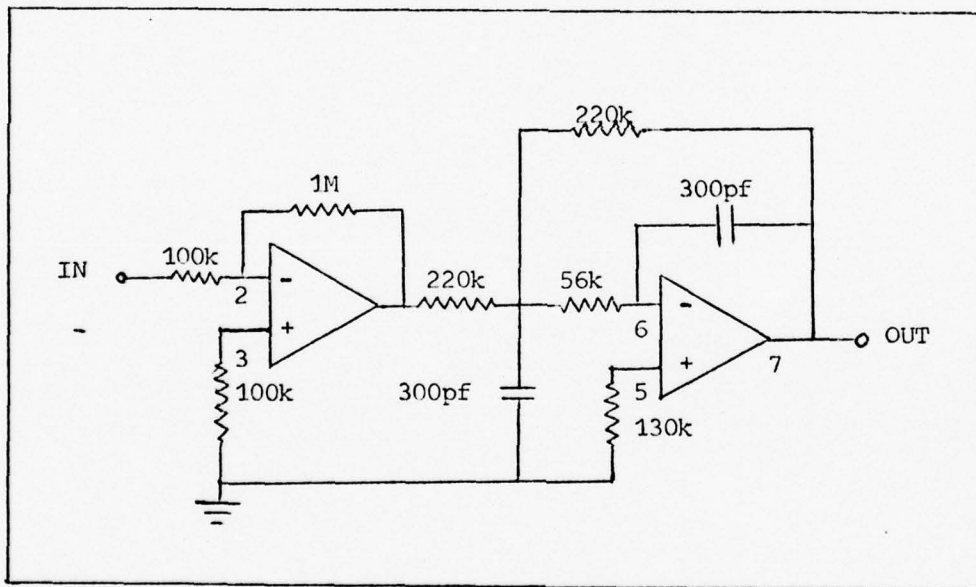


Fig. 7. Schematic of Bolus Box Preamplifier Circuit

to that described for the bolus counter used at Allison Division. The values in parentheses in Fig. 5 were the ones used on the bolus counter circuit at Wright-Patterson AFB. The RC time constant was set for 9 msec. This gave a dead time of 72 msec when the tape was played back at 15 ips since the tape was recorded at 1-7/8 ips. At 15 ips, a band-

of 10 to 1000 Hz was scanned by the pocket discriminating circuit. The square wave outputs from the pulse threshold circuits were amplified to produce a measurable signal at the chart recorder. The current traces and the positive and negative pulse indications were recorded on the strip chart recorder.

Initially this system was used with tape playback at 15 ips. This permitted a rapid scan to determine what was on the tape. This was the primary means of selecting those tapes which were studied in closer detail.

Engine Vibrations. Engine vibrations were studied using the system shown in Fig. 8. Only two Spectral Dynamics SD-101A frequency trackers were available. Therefore, the compressor and turbine vibrations were studied separately.

The first SD-101A was set up to examine the frequency spectrum of the vibrations. A sawtooth wave generator in the 7904 oscilloscope provided a signal which was used as a voltage ramp for the Wavetek 111 VCG voltage-to-frequency convertor. The output frequency of the VCG

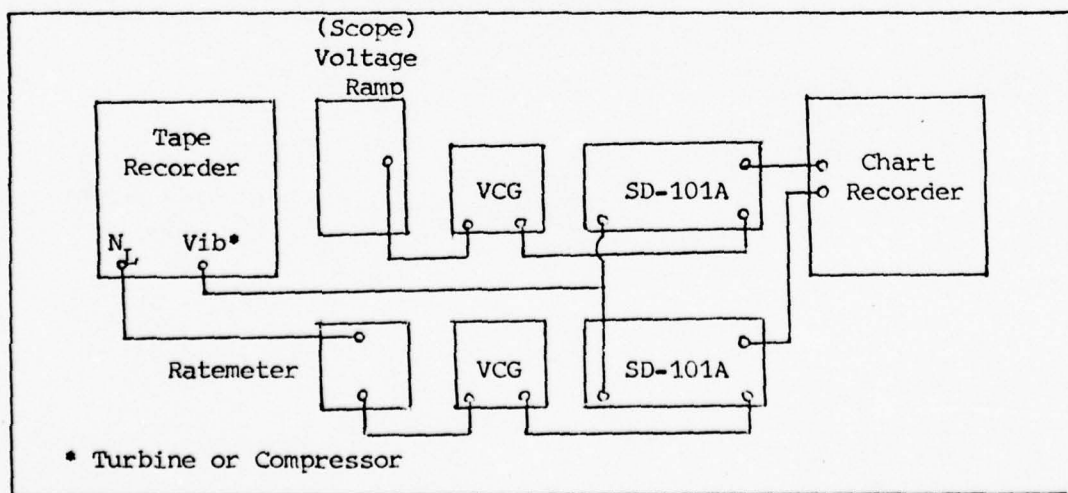


Fig. 8. Schematic of Vibration Analysis System

served as the tuning input to the SD-101A.

The second SD-101A was set up to examine the intensity of the N_L frequency. Since the recorded N_L was not a 1 to 1 ratio with the true engine N_L , the recorded signal had to be adjusted. This was done by placing the recorded signal into a Tennelec TC-590 ratemeter. The output of the ratemeter was amplified by a factor of 100 and then sent to a second Wavetek 111 VCG. The output of the ratemeter was converted into a frequency which approximated true engine N_L (approximately 1/3 of the recorded N_L signal). This was used as the tuning input for the second SD-101A.

The resultant signals from both SD-101A's were recorded on a strip chart recorder.

Photoanalysis. The shape and size of the pulse waveforms was studied using the system shown in Fig. 9.

Pulse rise above a threshold is normally used to trigger the oscilloscope. The sweep, however, will only show the pulse starting from the point at which it has triggered the oscilloscope. Thus no

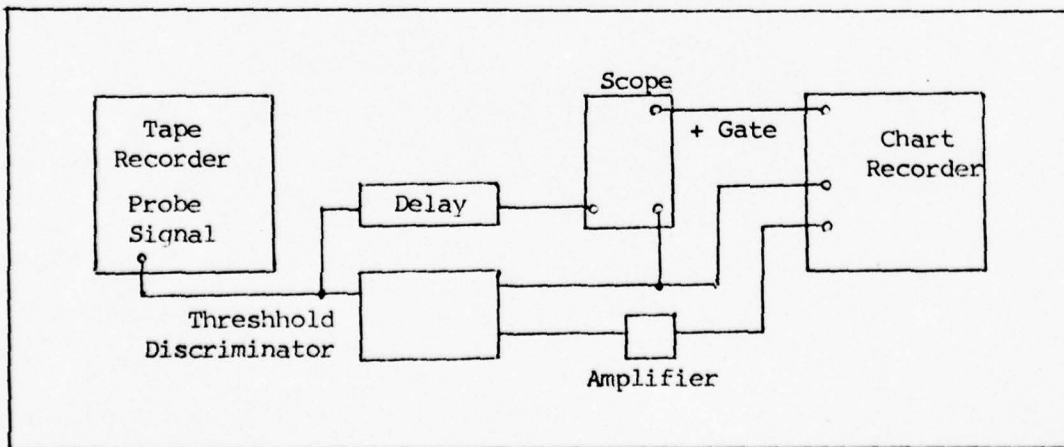


Fig. 9. Schematic of Photoanalysis System

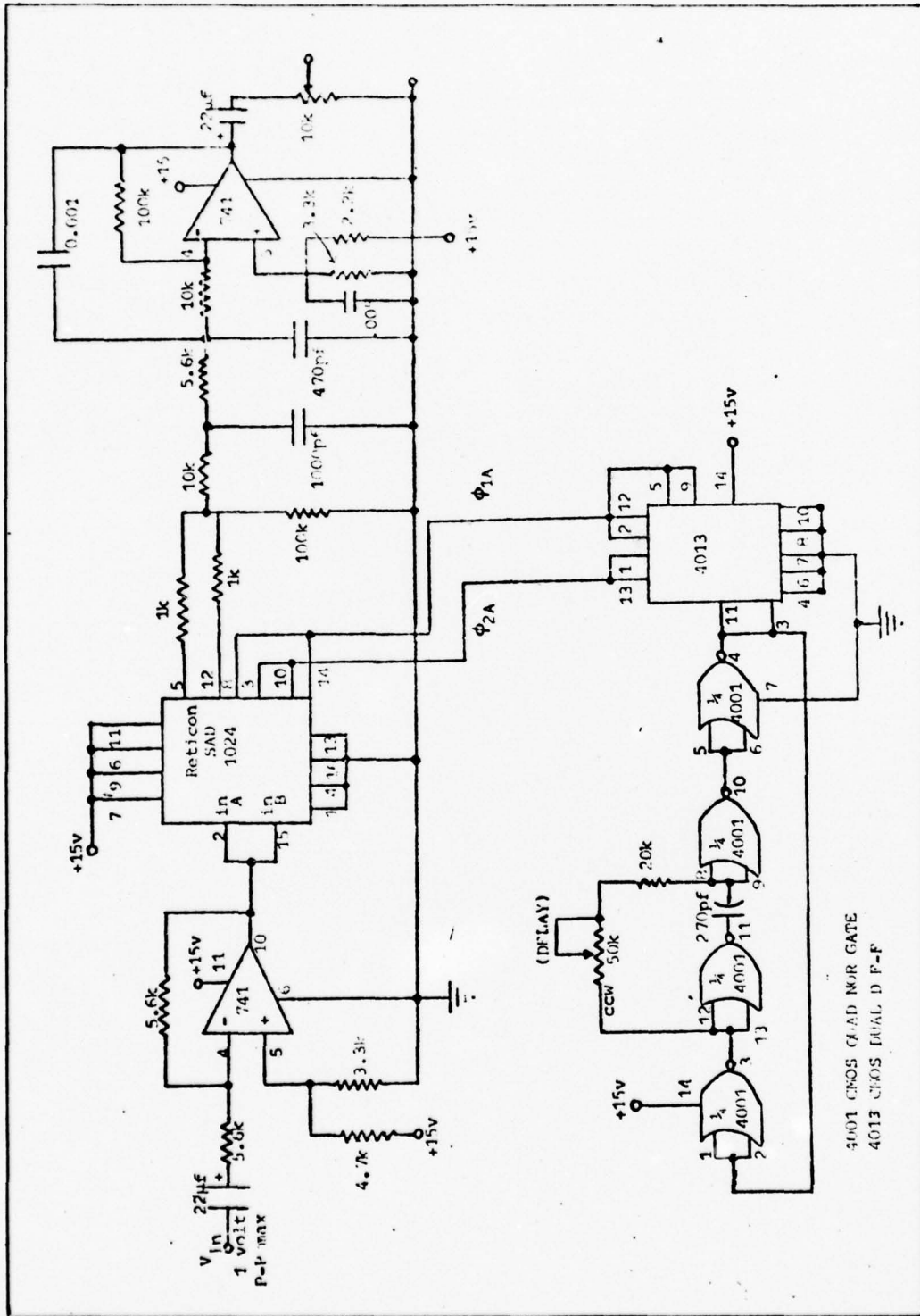


Fig. 10. Delay Box Circuit

information can be obtained from the current trace activity prior to the pulse. If pulses appeared at regular intervals, the oscilloscope could be set to trigger so that it would catch a pulse in the center of the screen. Since pulses appear on a random basis, a delay box was necessary to examine the complete pulse. The delay box circuit (Fig. 10) consisted of a Reticon SAD-1024 dual 512 stage Bucket-Brigade Device, a power supply, a 2.5 kHz low-pass filter, and an amplifier. Control knobs on the front of the box allowed the operator to adjust the amplitude of the delayed signal to agree with that of the input signal and to vary the delay from 4 msec to 14 msec.

The input signal to the delay box was kept below 1 volt to keep signal distortion below 1%. Since the signals were reduced by a factor of 10 before being recorded, this was no problem. The probe signal from the tape was the raw input to the delay box.

The delay box was AC coupled for design simplification. Normally, this did not cause signal distortion. On extremely long pulses, however, the coupling effect was observed (Fig. 11).

Since many pulses occurred close together in time, a method was developed to determine exactly which pulse out of a group had been photographed. The + Gate output of the 7904 oscilloscope provided a signal to the strip chart recorder. The pulse indication for the Gate lined up with the pulse indication for the particular pulse photographed.

Normally, pulses were photographed in real time. For extremely long pulses, however, the tape speed was increased to 7-1/2 ips. The pulse was squeezed together so that it could be photographed in its entirety. This also enabled the observer to see more of the current trace in front of the pulse.

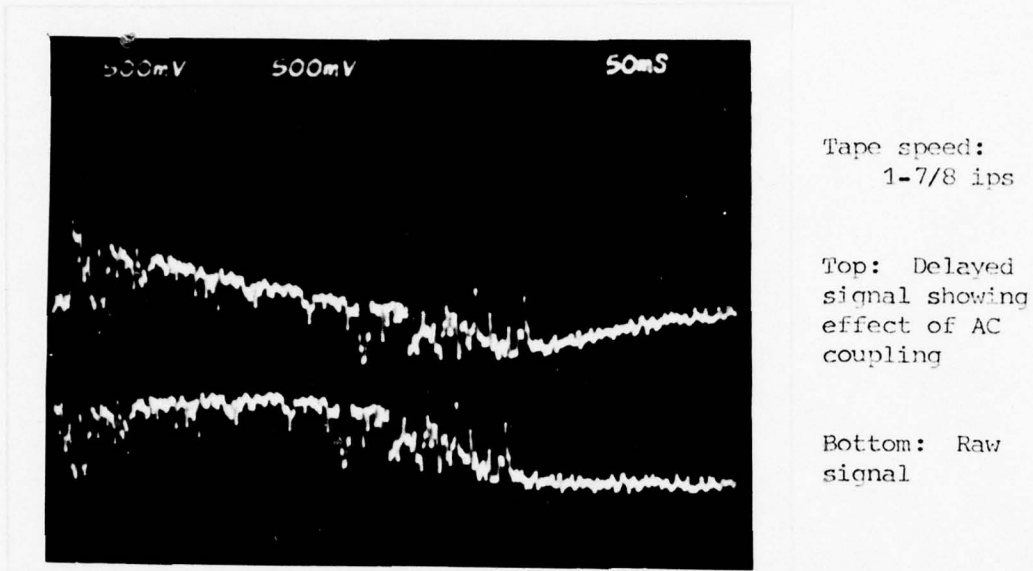


Fig. 11. Saturation Pulse Showing Effect of AC Coupling

Pulse Area Integration System. Studies of tapes recorded during severe microdistresses revealed that, in addition to the fact that there were more pulses, the pulses were wider than those observed in previous tests. If pulse width was a variable for all distresses, a system which integrated the area under a pulse might give a greater lead time for engine failure prediction.

The system shown in Fig. 12 was set up to check out the concept.

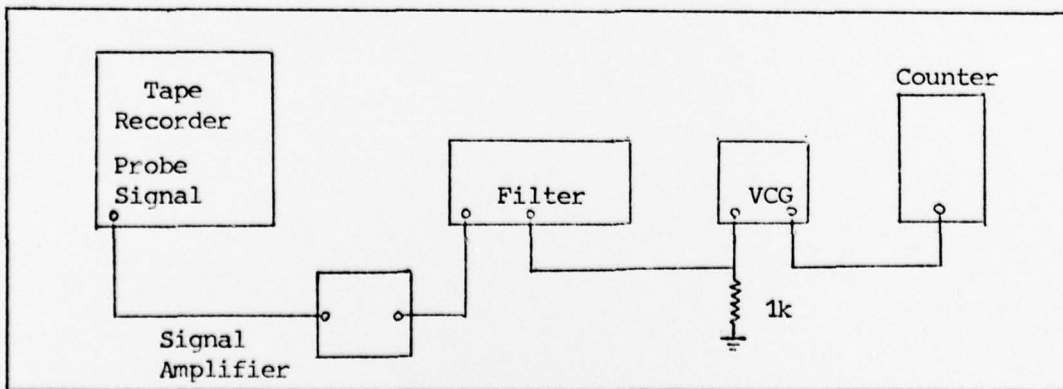


Fig. 12. Schematic of Pulse Area Integration System

After the probe signal was amplified by the bolus box preamplifier, it was AC coupled to a Dytronic Model 724 filter and high-passed at 1 Hz. A lower frequency would have been more desirable but 1 Hz provided little distortion. A -0.5 volt bias from the output DC level adjustment in the filter was used as a threshold to avoid counting background noise. The output of the filter was then sent to a Wavetek 111 VCG with a 1 k Ω resistance to ground. This was used to prevent saturation of the Wavetek 111. A 10 volt signal into the filter produced a 5.8 volt signal at the input of the Wavetek 111. The Wavetek 111 was used as a voltage controlled oscillator which produced signals at a rate proportional to the voltage applied. The signals were counted on a Tennelec TC-562P Timer/Scaler.

Total counts produced by a pulse were a function of the voltage (height) and time (width) and so gave a number that was proportional to the area of the pulse. Since the VCG would not operate with a negative

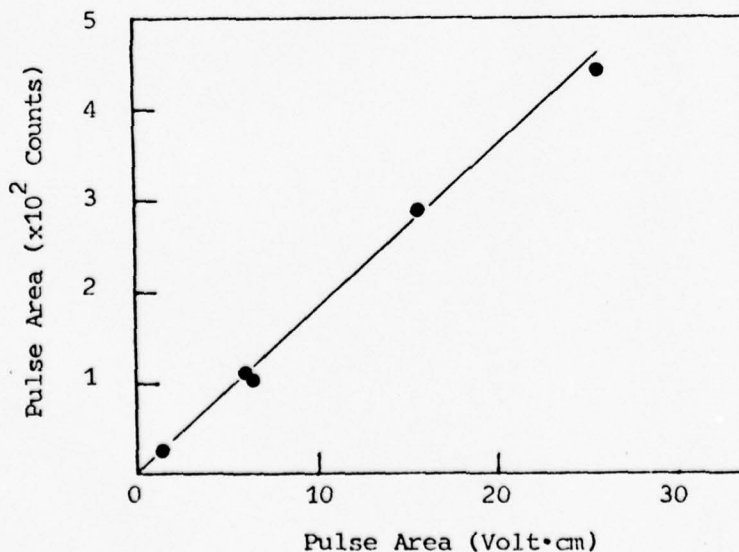


Fig. 13. Relation of Integrated Pulse Area Count to Actual Pulse Area

voltage input, only the areas of the positive lobes were counted.

The system was calibrated using single pulses from cycle A203. After the pulse was located, the photoanalysis system described in the previous section was used to photograph the pulse. At the same time, the pulse area integration system gave a count proportional to the area of that pulse. The results are shown in Fig. 13. A mean error of 6.7% between the pulse area and the count was found. This was considered to be acceptable since a factor of 2 above background was expected.

Limitations

Some data was lost during this test. The first reason was equipment malfunction. There was only one tape recorder available. The tape drive malfunctioned and the tapes it produced were unusable. Loose or broken cables from the probes to the bolus box also caused data loss. The cause for this malfunction was most likely personnel in the test stand area servicing the engine.

A second reason for data loss was that the tapes were not always changed when one tape was filled. During weekdays, tape changeover went fairly well. On weekends and at night, however, the system broke down. The one non-catastrophic failure occurred during the period from 24 June to 28 June. Many of the cycles run during this time were not recorded because the tape was not changed. The bolus counter operated independently of the tape system, however. Thus, although not all of the cycles were recorded, the count history provided a relative magnitude of distress during that period.

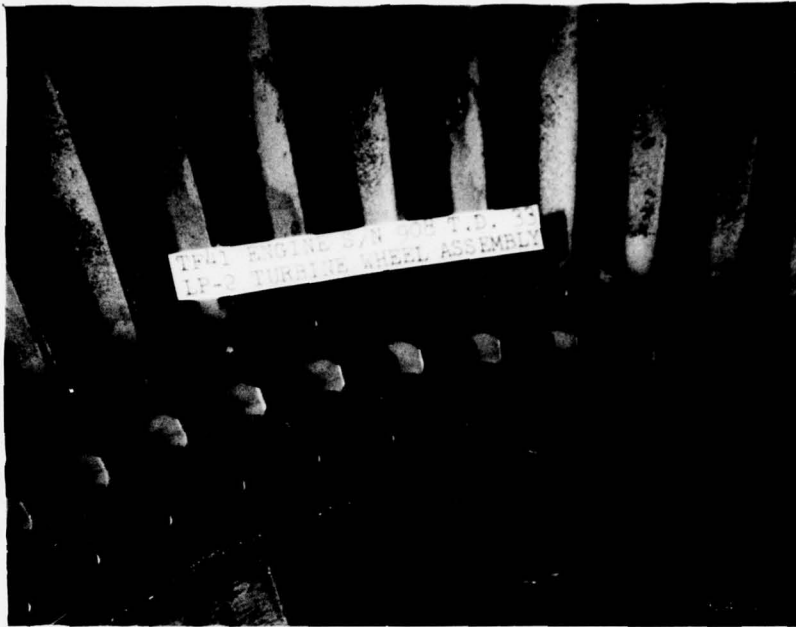
III. Experimental Results

The purpose of this chapter is to provide a description and discussion of the experimental results. There were four major areas of investigation: probe current traces as indications of engine stress, vibrations, individual pulse recognition, and pulse area integration. The A cycles provided most of the data discussed in this section. Some C cycles were used, however, to show a thrust-current level relation. For purposes of this discussion, the A cycle can be divided into five regions: Beginning (B), Severe Transients (ST), Moderate Transients (MT), High Power Steady State (HPSS), and End (E). Refer to Appendix B for diagrams of the A and C cycle profiles.

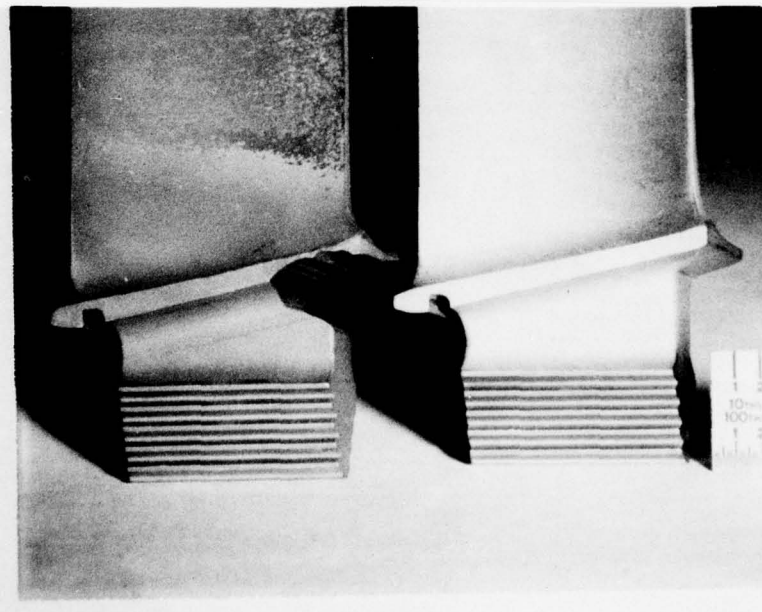
Tapes recorded between 24 June and 28 June indicated that the engine had undergone an unusual distress. The counts produced by the bolus counting system at Allison Division showed that the number of positive counts increased by a factor of 2 while that of the negative counts increased by a factor of 100. See Appendix D.

Although the nature of the distress could not be determined by the electrostatic probe system, there was little doubt that something had happened to the engine.

Large pulses (350 msec long, 8 volts high) were first noted on accelerations during the ST period of cycle A181. They were seen by the 2:30 probe. They were not seen again until cycle A203, about 19 test hours later. This time they were seen by both probes. They also appeared on cycles A204 and A205 which immediately followed A203. In addition to appearing on accelerations during ST, the pulses were seen



(a)



(b)

Fig. 14. LP2 Turbine Damage (TF-41 S/N 908)
(a) Section of Turbine Wheel Assembly
(b) Detail of Single Turbine Blade

on accelerations during MT. Whether the pulses appeared in cycles immediately after this is not positively known since the tape was not changed. The bolus counter at Allison Division, which ran independently of the tape recorder, showed that positive and negative count rates similar to those found on cycles with the large pulses did, in fact, occur on cycles which were not recorded on tape.

The first teardown after this series of cycles did not reveal any significant wear. The low pressure (LP) turbine section was not examined, however. The engine was rebuilt and put through another series of cycles. No significant pulse rates were observed. On the next teardown, the LP turbine section was examined. A large gash was found in the turbine blade stems around the entire LP2 turbine wheel (Fig. 14). The gash was 0.3 in. deep.

The cause of the damage was an aft seal which had slipped forward and rubbed along a 50° arc, from the 2:00 to the 3:30 o'clock position, on the seal. As the turbine wheel rotated, this 50° portion of the seal rubbed the groove into the turbine. After a sufficient amount of the turbine assembly had worn away, the seal no longer made contact and the rubbing stopped.

Allison engineers could not determine when the seal had started or stopped rubbing.

Probe Current Traces as an Indication of Stress

The HPSS regions of A cycles were used to establish a relationship between the probe current trace and T_1 . The trace recorded on a strip chart showed that the magnitude of the DC level above a zero reference varied inversely with T_1 (Fig. 15). The temperature was not rigidly controlled during the tests so only an approximate relationship could

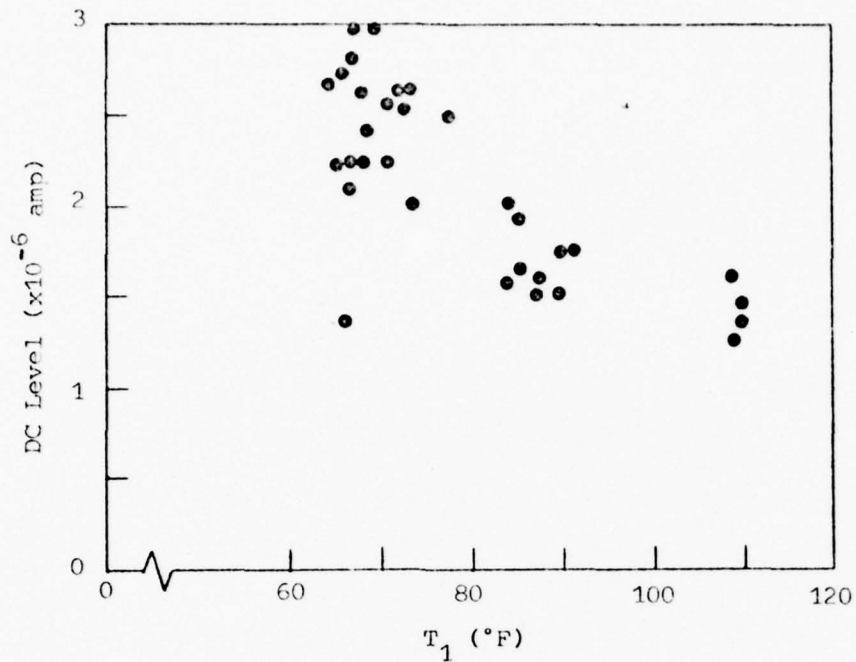


Fig. 15. DC Level as a Function of T_1

be seen.

The current level was also found to vary directly with gross engine thrust. Four C cycles from Build 31 were used to check this rela-

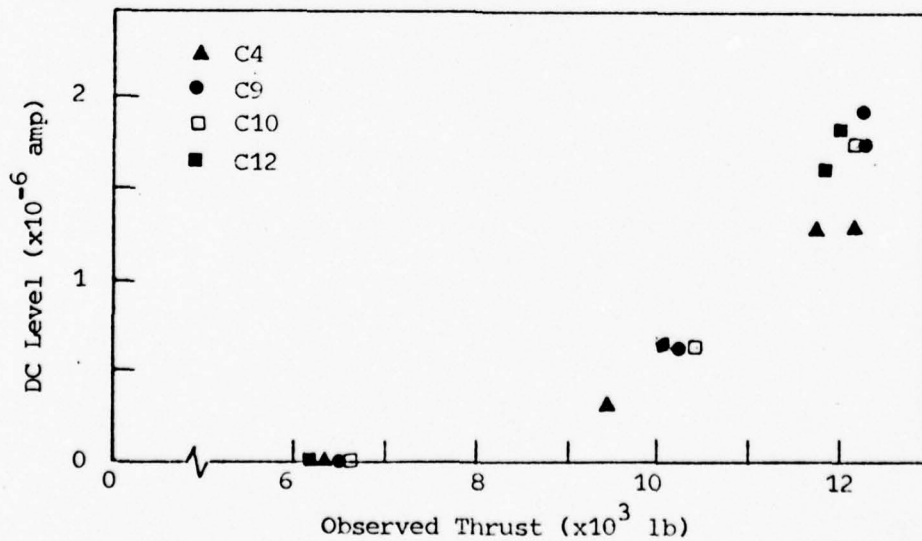


Fig. 16. DC Level as a Function of Gross Thrust for TF-41 S/N 908

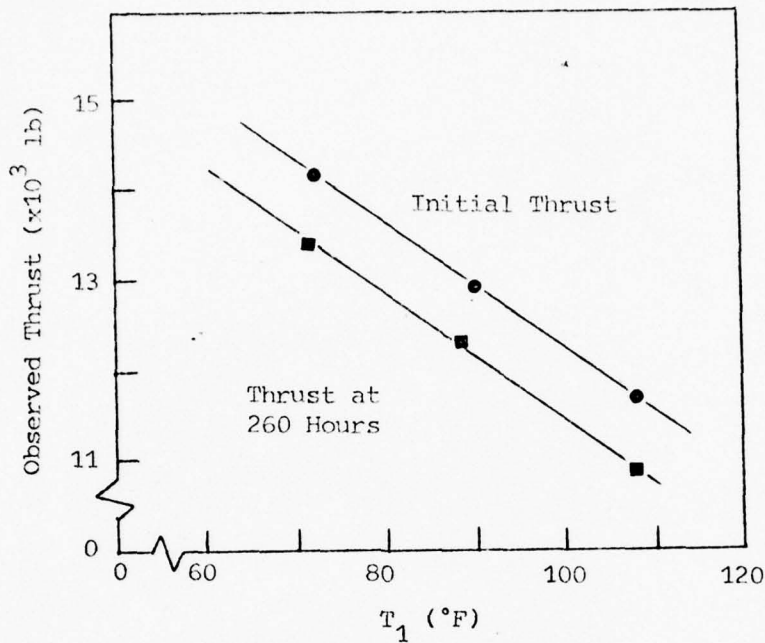


Fig. 17. Thrust vs T_1 for TF-41 S/N 908

tionship. The current levels at each thrust setting (Intermediate, 95%, and 90%) were averaged and plotted against the observed thrust for that portion of the cycle (Fig. 16).

The number of background pulses produced by the engine varied inversely with T_1 . Qualitatively, this made sense. Thrust is inversely proportional to T_1 (Fig. 17). As the temperature decreased, the engine worked harder and was more susceptible to microdistresses. During normal engine operation, then, boluses were produced at a rate that was a function of thrust. When a severe microdistress occurred, however, the boluses were produced at a rate considerably above the background rate.

Fig. 18 shows the number of boluses detected as a function of current during HPSS. In order to obtain a current level more representative of the whole exhaust, the levels for the 2:30 and 6:30 probes were averaged. The counts obtained by each probe were added together. The

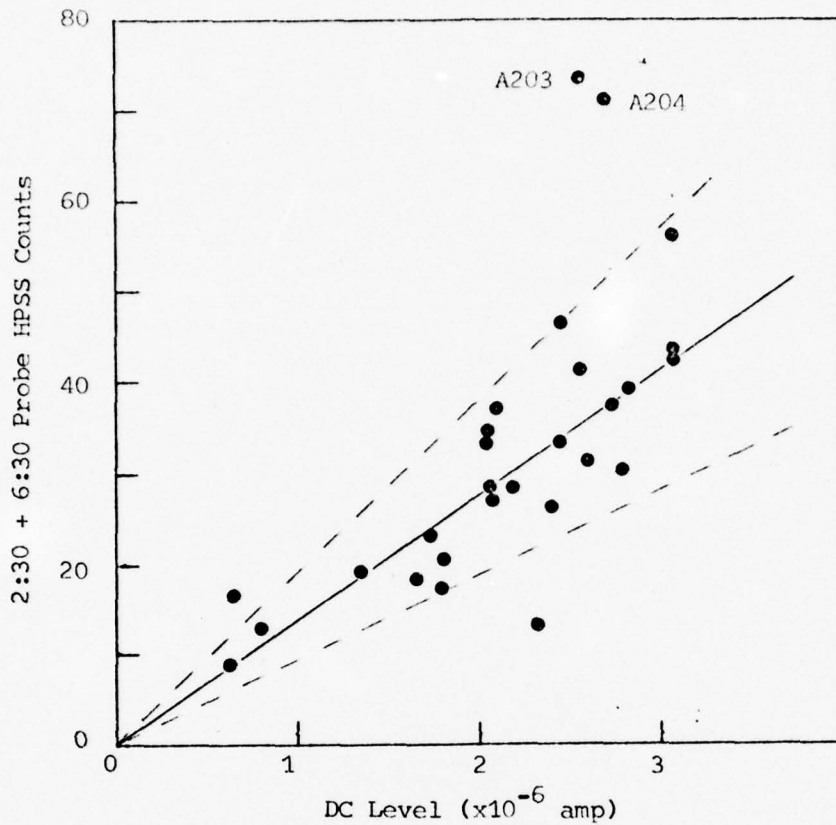


Fig. 18. Pulse Count vs Average HPSS DC Level of 2:30 and 6:30 Probes in TF-41 S/N 908

tape was played at 15 ips so some boluses were presumably lost due to the RC dead time of the bolus counter circuit. The number of counts for cycles A203 and A204 were approximately twice that of the mean for their particular DC levels.

Vibrations

A frequency scan of the turbine and compressor vibrations at HPSS indicated that a mechanical change in the engine had taken place during the period in which the large pulses occurred. This change was indicated by the relative amplitudes of the peaks in the frequency spectrum.

The primary peak in both turbine and compressor vibration spectra

during HPSS was $N_L = 146$ Hz. Peaks at $N_H = 213$ Hz and $2N_L = 293$ Hz were also seen.

Compressor. The compressor vibration spectrum remained essentially unchanged from the earliest cycle recorded (A61) through A190, a period of 98 hours. The amplitudes of N_H , $2N_L$, and an undefined peak at 241 Hz fluctuated during the period from A190 through A205, a period of 15 hours. This was the period in which numerous large pulses were seen. The next available data came from A246, 32 hours later. At that point, the four peaks had stabilized. The N_L peak amplitude had a general downward trend with the exception of cycles A251 through A255. After A255, N_L decreased to about one-half its value prior to the onset of the large saturation pulses. See Fig. 19.

Turbine. The turbine vibration spectrum did not change until A181. At that point the amplitude of N_L increased by 1/3. On the following cycle, however, it returned to its original value. N_L again increased during cycles A203 and A205. N_L amplitude remained elevated in cycles A246 and A247 but returned to its original value in A248. The $2N_L$ peak amplitude dropped by a factor of three during A256 and did not increase again. See Fig. 20. Due to time considerations and equipment limitations, a complete check of turbine spectra through A283 was not made. Up to the point where examination of turbine spectra stopped, however, there was a downward trend in N_L amplitude.

An attempt was made to correlate pulse signals with blade strikes or tip rubs in the turbine area. It was theorized that a mechanical rub might produce a change in the amplitude of certain frequencies in the turbine vibrations. No changes were observed in frequencies at N_L or N_H . The raw vibration signals were put through a filter and an RMS

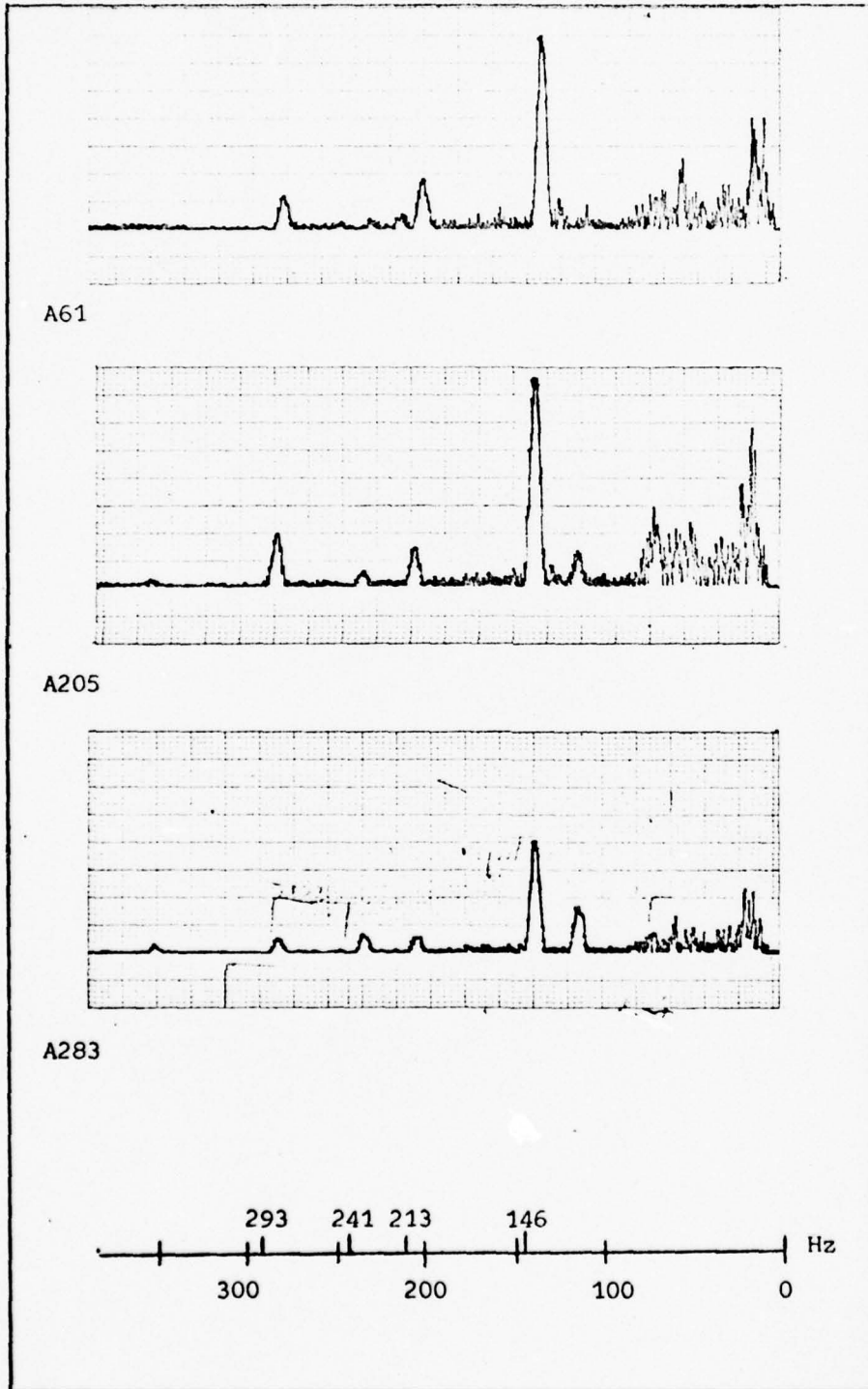


Fig. 19. Compressor Vibration Frequency Spectrum

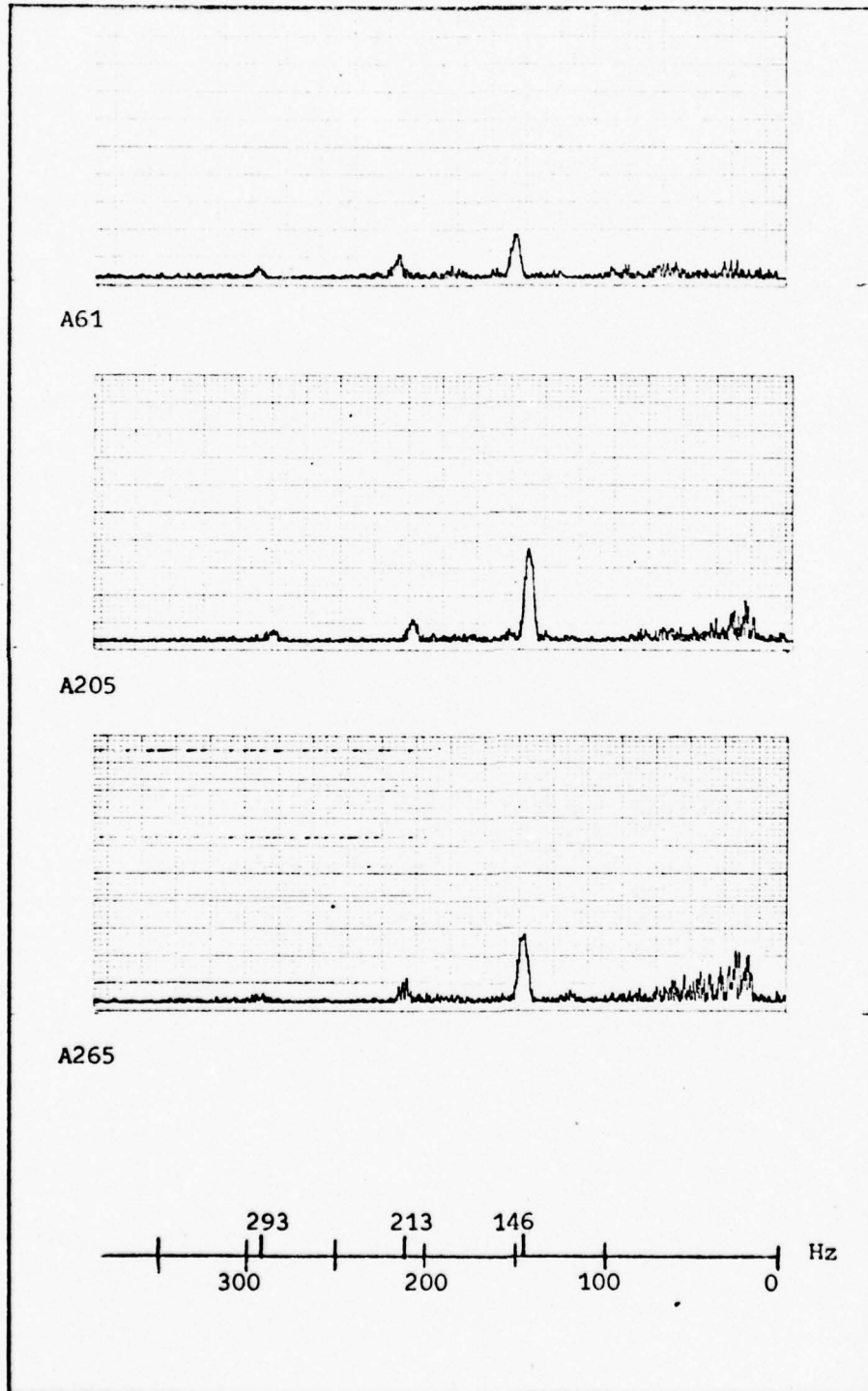


Fig. 20. Turbine Vibration Frequency Spectrum

voltmeter before being recorded on the strip chart recorder. The signals were band-passed at frequencies ranging up to 600 Hz. No correlations were observed.

Photoanalysis

Pulses were photographed using the delay box system described in the previous chapter. The pulses fell into three basic categories: bipolar (having both positive and negative components), positive monopolar (having a positive component only), and saturation. The pulses were photographed using the raw signal from the tape recorder as the input to the delay circuit. Thus the amplitudes shown in the photographs are 1/10 the amplitude of the actual pulses. Allison personnel who recorded the data took photographs of the signal as it came from the probe and after it was recorded and verified this reduction factor, as well as the recorder reproduction fidelity. Thus, the reader can determine the true pulse amplitude by multiplying the displayed vertical scale by 10. With the exception of the saturation pulse photograph all photographs were made using a playback speed of 1-7/8 ips so that the horizontal scale is correct. A tape speed of 7-1/2 ips was used to photograph the saturation pulse. Therefore, the displayed horizontal scale must be multiplied by 4.

Bipolar pulses (Fig. 21) had been observed during previous engine tests. The pulses were about 5 msec wide with a maximum amplitude of 8 volts positive and 3 volts negative.

The positive monopolar pulses (Fig. 22), which had also been observed on previous tests, varied considerably in width but were approximately 8 volts high. The width of these pulses varied from 3 to 10

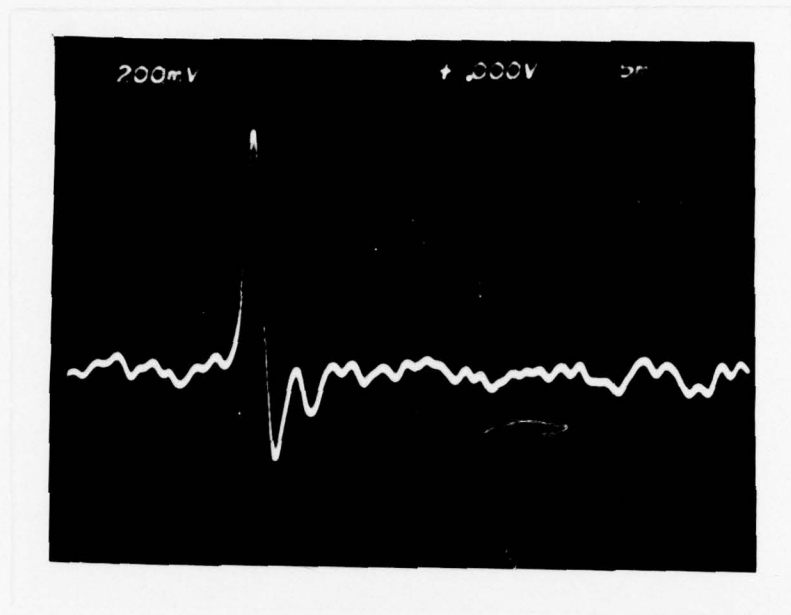


Fig. 21. Bipolar Pulse

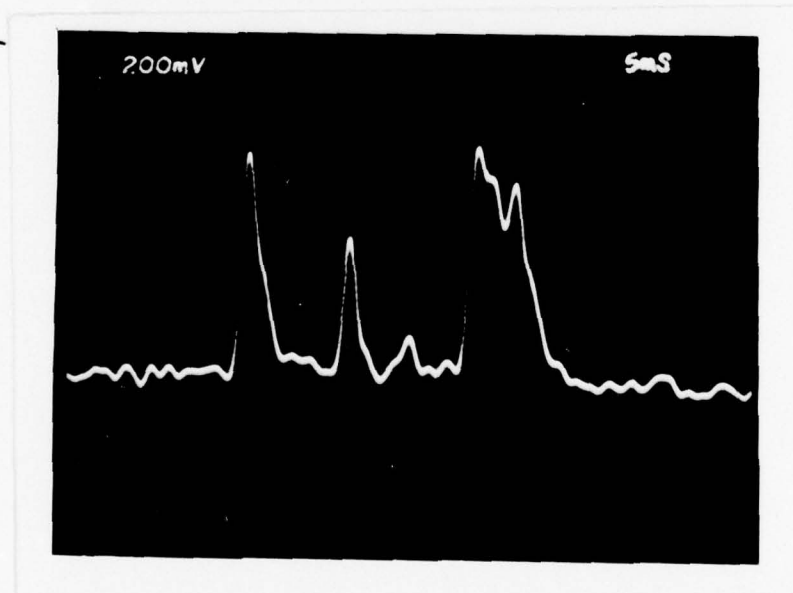
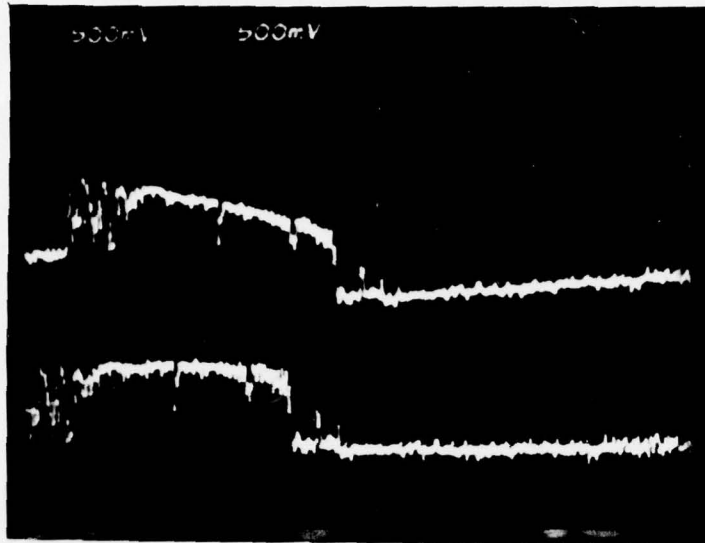


Fig. 22. Series of Monopolar Pulses



Tape speed:
7-1/2 ips

Top: Delayed
trace

Bottom: Raw
trace

Fig. 23. Saturation Pulse

msec. Often, the narrower pulses occurred in groups.

The saturation pulses (Fig. 23) occurred on cycles A181, A203 through A205, and occasional cycles through A284. They were produced during accelerations, especially during the ST portion of the cycle. They were 320 to 380 msec wide and 8 volts or more high.

Pulse Area Integration System

The pulse area integration system was tested using A cycles which had been checked using the conventional pulse counting system. Under the conventional system A204 stood out from the background by a factor of 2 while under the new system it stood out by a factor of 20 on the 2:30 probe and by a factor of 8 on the 6:30 probe (Fig. 24).

During the cycles in which the saturation pulses occurred, the

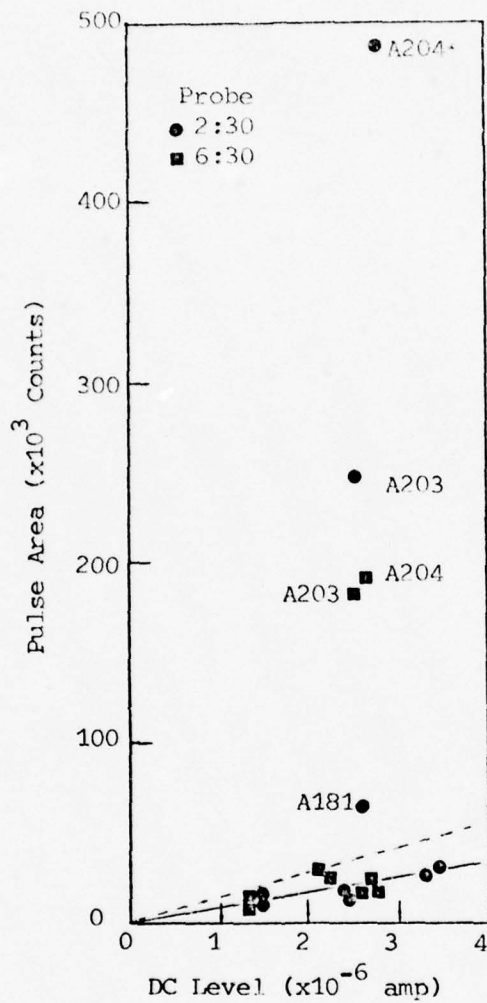


Fig. 24. Pulse Integrated Area Count vs HPSS DC Level

2:30 probe consistently gave a higher count. Since the count was proportional to the area under the pulses, the 2:30 probe interacted with more and/or larger boluses than did the 6:30 probe during this time.

Cycle A181, in which the saturation pulses were first observed, had an unusually high count on the 2:30 probe. It stood out from the background by a factor of 3. The 6:30 probe had a count within background range. Thus the 2:30 probe indicated unusual activity first.

IV. Conclusions and Recommendations

The purpose of this chapter is to summarize the conclusions of this study and to give recommendations for ways to improve engine stress monitoring and data analysis.

Conclusions

With minor modifications, the systems discussed in this paper can be used efficiently to sort out those tapes which deviate from a background data base. This can enable the observer to test more than one engine at a time and so have a greater probability of seeing an engine failure.

An inverse relation between T_1 and the number of pulses generated by the engine has been observed. This tends to confirm the evidence that bolus formation is stress related and increases as T_1 decreases (or as thrust increases).

A relation has also been observed between the DC level of the current trace and gross engine thrust. The data points were too scattered to determine the exact shape of the curve. This was probably due to the variation of T_1 during the measurement period and to probe design. Also, the two probes measured only a small portion of the exhaust.

A change in vibration signature in the turbine and compressor vibrations was seen. At the time that this change took place, large pulses were detected by the probes.

A probability that the systems detected and recorded the LP2 rub can be estimated using the data found in Appendix C. Since there is a 0.83 probability that high counts associate with a failure/distress,

there is a 0.17 chance that the high counts detected during this test were not an indication of the observed failure. The probability that the 2:30 probe randomly counted more than the 6:30 probe is calculated in the following manner. The probability that one probe was in front of the 50° distress site is $50^\circ/360^\circ$ or about 0.14. The probability that at least one probe was in front of the distress site is 0.28. Therefore, the probability that one probe, at least, was not in front of the distress site is 0.72. The probability that one probe randomly had a higher count is 0.5. Thus, the probability that the 2:30 probe counted more boluses than the 6:30 probe for only random reasons is 0.72×0.5 or 0.36. The probability that the vibration signature of the engine randomly changed during this period is, conservatively, 0.5. The probability that all of these things occurred randomly at the same time is the product of the individual probabilities, or 0.03. Since the probability of correlation plus the probability of non-correlation (random events) is unity, the probability that these events relate to the observed distress is 0.97.

Recommendations

Since an electrostatic ring has been shown to produce valuable data, it should be installed on the engine and tested with the systems described in this paper. The ring would provide more quantitative data with which the net charge produced by a distress could be calculated.

The probe system should be modified so that a greater area of the exhaust is sampled. A probe system consisting of a loosely-woven wire mesh in the exhaust stream is one possibility. With the present system results can vary due to the distance of the bolus from the probe as it passes the plane of the probe.

The DC level of the current trace should be studied at rigidly controlled inlet temperatures and thrust settings. The probe system could, with modification in design, have an application as a gross thrust indicator.

Recorded N_L and N_H should have a 1:1 ratio with actual N_L and N_H . This would simplify vibration level tracking. In addition, a two- or three-axis higher frequency vibrometer would furnish additional data for correlation of pulses with blade strikes or tip rubs.

The pulse area integration system should be developed further. This system provides a number proportional to the area under the pulses it measures. It could be set up as a real-time engine stress indicator. The system should be built such that it automatically starts integrating at the beginning of the cycle. At the end of the cycle, it should print out the count and zero itself. The printout could be examined to determine cycles with unusually high counts. These cycles could then be studied in greater detail. Whether the cycle contained more pulses or larger pulses would not be known from the total count. This problem could be solved by a more advanced system with circuits to store data on pulses with specific heights and/or widths in memory and print the results at the completion of the cycle.

Bibliography

1. Arlen, Richard E. An Investigation of Laser-Target Interaction Signals. Unpublished Thesis. Wright-Patterson Air Force Base, Ohio: Air Force Institute of Technology, December 1975.
2. Burgess, Ray W. An Investigation of the Detection of Charged Metal Particles in a Jet Engine Exhaust by a Cylindrical Electrostatic Probe. Thesis. AD745540. Wright-Patterson Air Force Base, Ohio: Air Force Institute of Technology, June 1972.
3. Couch, R. P., and Molnar, T. Presentation to 1975 IEEE Plasma Science Conference. Ann Arbor, 14 May 1975.
4. Couch, R. P., and Poch, R. C. An Ion Probe to Predict Failures in Jet Engines. 8th Annual FAA International Aviation Maintenance Symposium, November 1972.
5. Dunn, Robert W. The Electrostatic Sensing of Simulated MA-1A Gas-Path Distress. Unpublished Thesis. Wright-Patterson Air Force Base, Ohio: Air Force Institute of Technology, December 1976.
6. Hill, Gail E. Imminent Engine Failure Probe Investigation. AFAPL TR-74-30. Wright-Patterson Air Force Base, Ohio: Air Force Aero Propulsion Laboratory, 1974.
7. Mitchell, John E. Exploding Wire Simulation of Jet-Engine Gas-Path Microdistresses. Unpublished Thesis. Wright-Patterson Air Force Base, Ohio: Air Force Institute of Technology, December 1975.
8. Shaeffer, J. F., and Peng, T. C. High-Potential Clouds in Jet-Engine Exhausts. 9th Fluid and Plasma Dynamics Meeting of the American Institute of Aeronautics and Astronautics. San Diego, July 1976.

Appendix A

Theory of Bolus Formation

Since it is a documented experimental fact that pockets of charge (boluses) do exist in the exhaust of jet engines (Ref 8), the theory is restricted to how the boluses are made by distresses.

The bolus is thought to have two possible sources. The first is a mechanical rub between two components in either the compressor or turbine section of the engine. The second possible source is an overheat condition which causes microscopic pieces of metal to separate from the components in the combustor section.

Mechanical Rubs

Initially a rub bolus is composed of metal particles in a plasma. The particles pick up a negative charge due to the high random current of electrons but the bolus has no net charge. As the bolus moves through the gas-path, however, the metal particles collide with obstructions such as guide vanes and turbine blades. The larger particles either embed themselves in, or transfer their charge to, these obstructions. The remaining bolus of ions and/or small charged particles, lacking the inertia of the more massive particles, passes through the gas-path without colliding with the various engine components. The bolus now has a net positive charge. When the bolus enters the tail-pipe and passes an electrostatic probe, there is an interaction which registers as a positive pulse on the probe current trace.

Combustor Burns

Burns also produce a bolus composed of metal particles and plasma. The temperature of the burn, however, affects the polarity of the pulse produced (Ref 7:43-44).

If the temperature is approximately at the melting point of the material, the bolus will act like a rub bolus: that is, a positive pulse will result.

If the temperature is high enough for the metal particles to thermionically emit electrons, the metal particles will have a net positive charge when they are deposited on the engine obstructions. This will leave a net negative charge in the bolus. The bolus will then produce a negative pulse on the probe current trace.

Appendix B

Profiles of A and C Cycles

A Cycle

The A cycle consisted of a series of accelerations and decelerations with periods of high power steady RPM operation. It lasted approximately 43 minutes.

Fig. B-1 was made by recording N_L on the strip chart recorder. The tape was played at 15 ips. Chart speed was 1 mm/sec. Time increases from right to left. The approximate RPM settings are indicated on the right of the figure. Increasing time in minutes is indicated at the bottom. The five regions called Beginning (B), Severe Transient (ST), Moderate Transient (MT), High Power Steady State (HPSS), and End (E) are arbitrary designations. They are used only to narrow the region of discussion.

C Cycle

The C cycle consisted of a series of accelerations to a high power steady RPM plateau and subsequent decelerations. Three RPM settings were used: Intermediate (Full Thrust), 95%, and 90%. The cycle consisted of six accelerations to Intermediate, five acceleration to 95%, four accelerations to 90%, and finally five more accelerations to Intermediate. The Intermediate power settings were held for 3.25 minutes. All other power settings were held for 3 minutes. The time between one deceleration and the next acceleration was 3 minutes.

Fig. B-2 was drawn to show the cycle profile. Time again reads

from right to left. The approximate RPM settings are shown on the right.

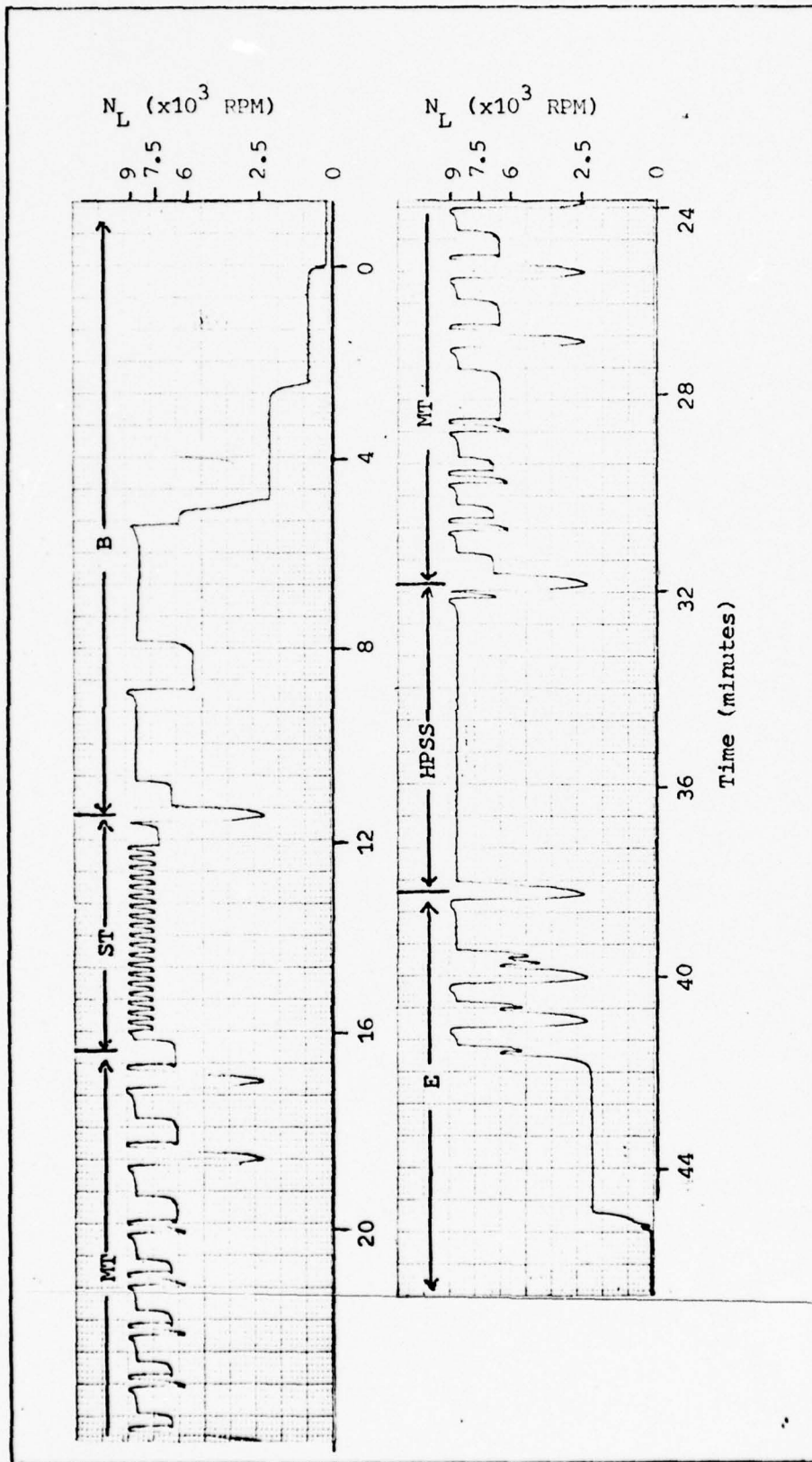


Fig. B-1. Profile of A cycle

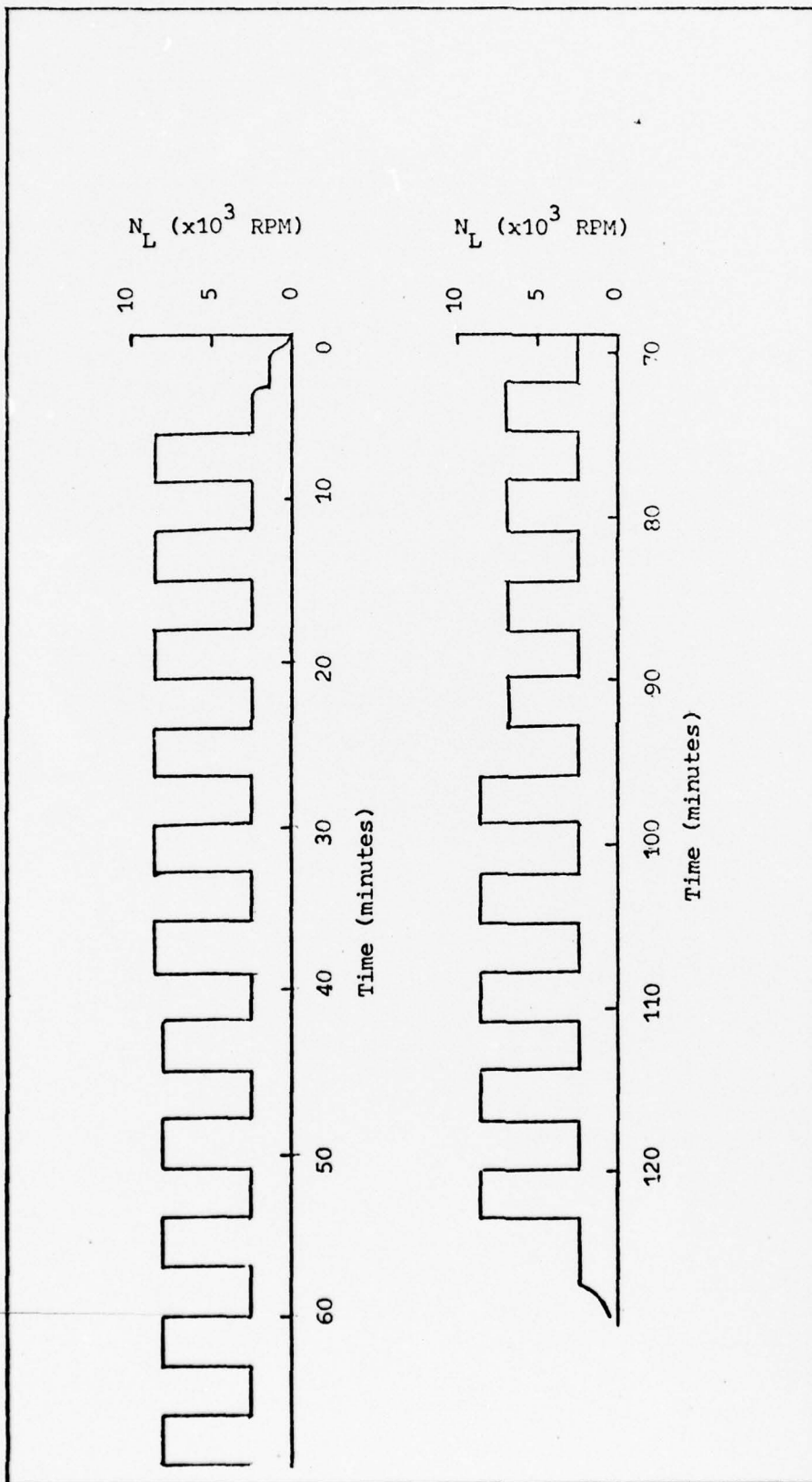


Fig. B-2. Profile of C cycle

Appendix C

TF-41 Failure History

The figures which follow are taken from Ref 6 and unpublished notes of a briefing presented by Major Couch. They are based upon approximately 2300 hours of testing prior to the event discussed in this study.

It can be seen (Fig. C-1) that high counts have a definite correlation with failures and distresses. Of seven observed failures (or distresses) five were predicted. Of six tests with high counts, five correlated with failure.

Fig. C-2 through C-6 give the count histories for the engines which enter into the failure matrix.

	Failure/Distress	No Distress
High Count	5	1
Low Count	2	Most data uneventful

Fig. C-1. Failure Correlation Matrix

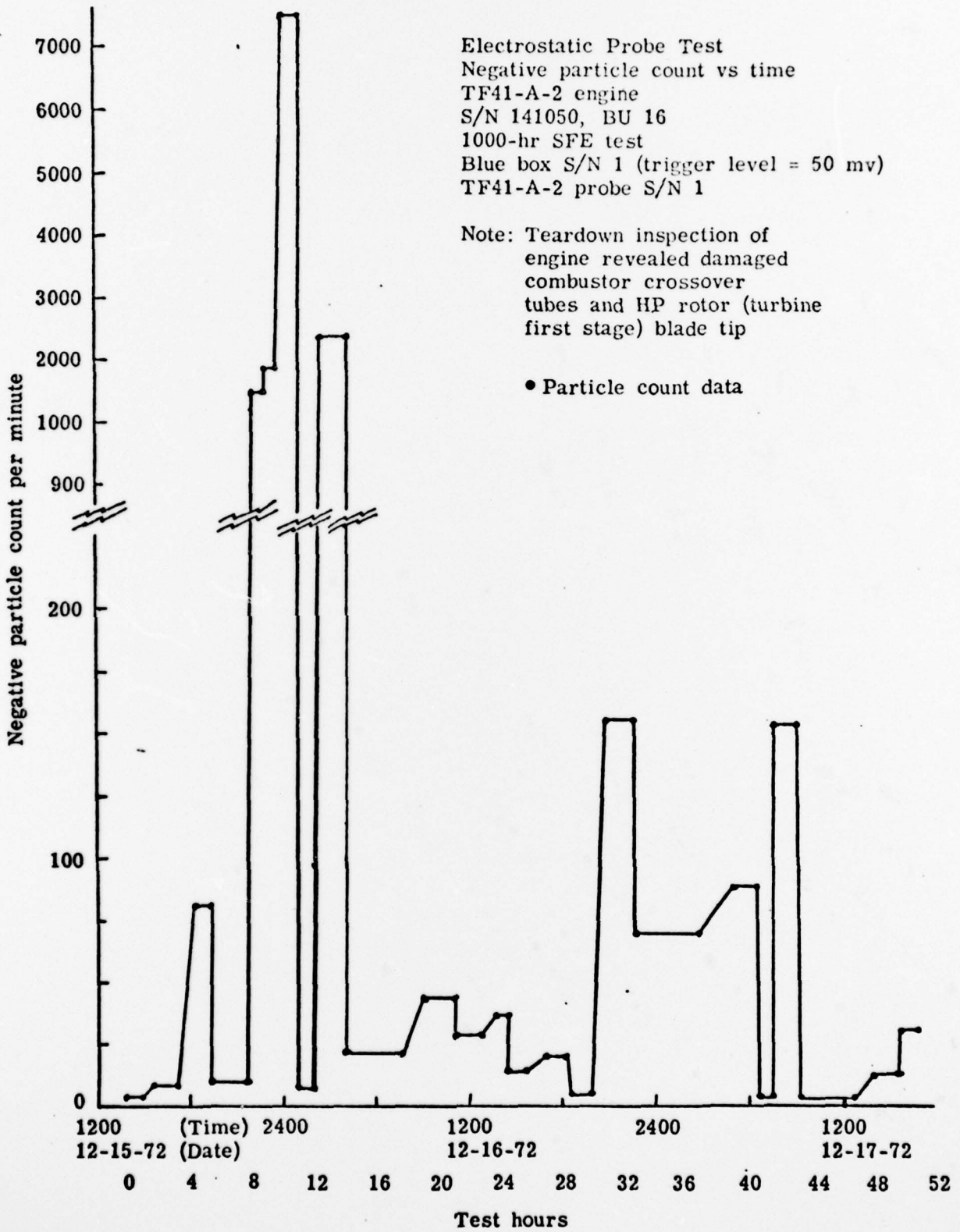


Fig. C-2. TF-41 S/N 141050 (B.U. 16) Particle Count vs Time (Ref 6:60)

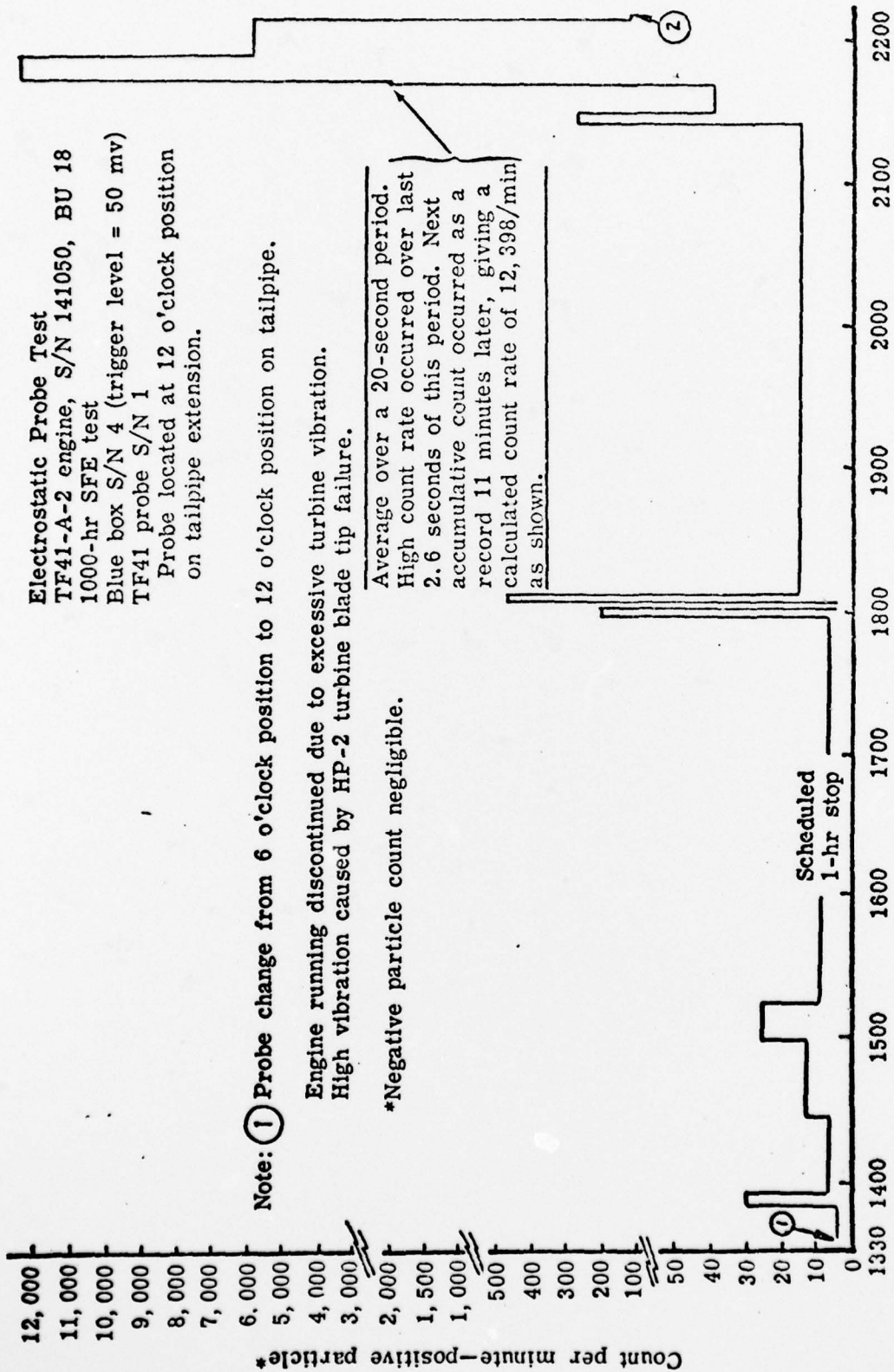


FIGURE C-3. TF41-A-2 Engine No. 141050 (B.U. 18) Particle Count Vs. Time (Ref 6:65)

TF41 engine, S/N 908, BU 25, 26, & 27
 Blue box S/N 2 (trigger level = 50 mv)
 TF41 probe S/N 2 (7 o'clock position on tailpipe extension)

Notes:

1. BU 25, end of testing. Replaced LP compressor front seal and seal rings because of excessive wear (high oil consumption and vibration).
2. BU 26, start of testing.
3. BU 26, end of testing. LP-2 turbine blade failure. Replaced damaged parts.
4. BU 27, start of testing.
5. BU 27, completion of engine testing.

Date of engine testing was Sept 14, 1973 through Oct. 10, 1973.

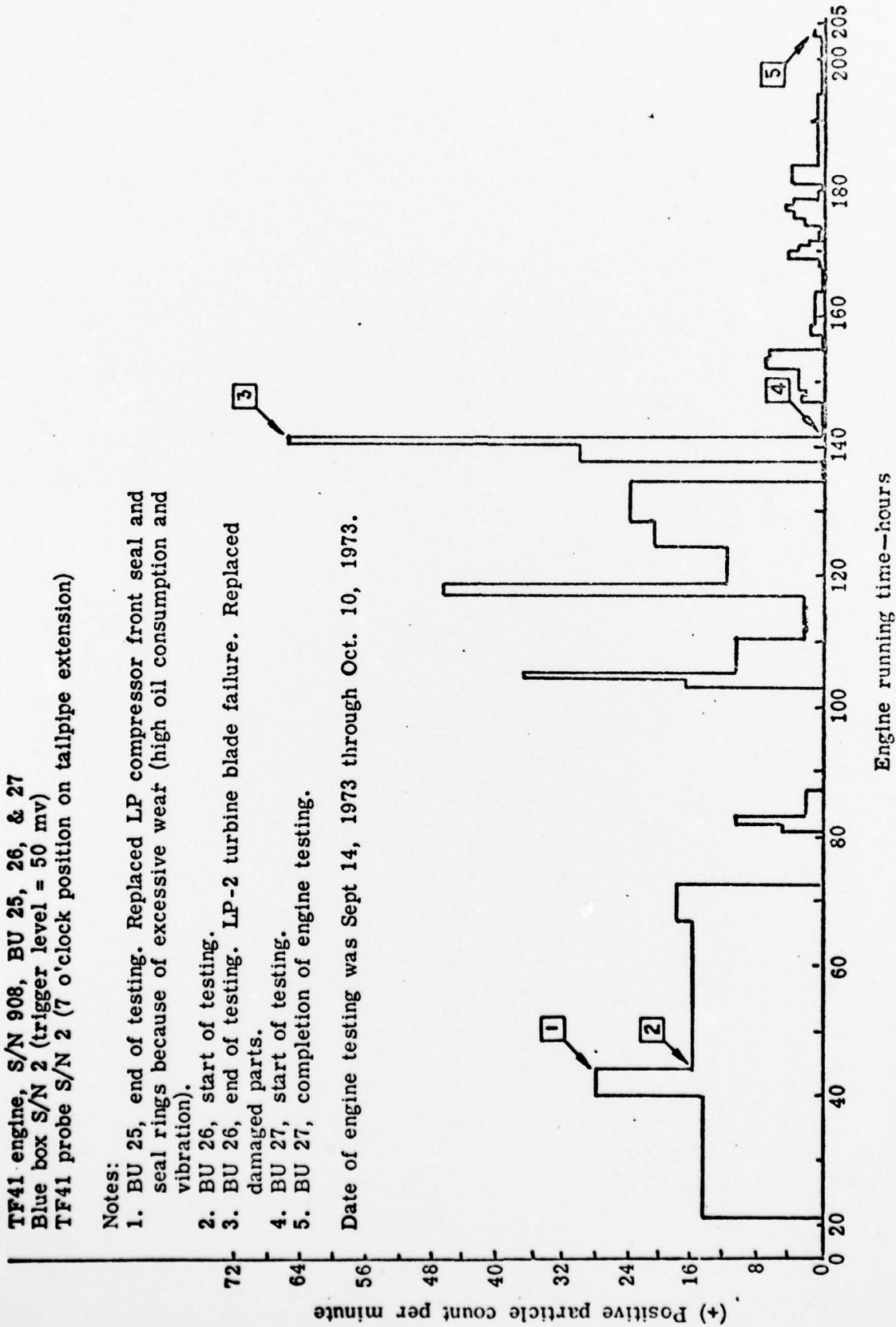


FIGURE C-4. Electrostatic Probe Test - (+) Positive Particle Count Vs. Engine Running Hours (Ref 6:71)

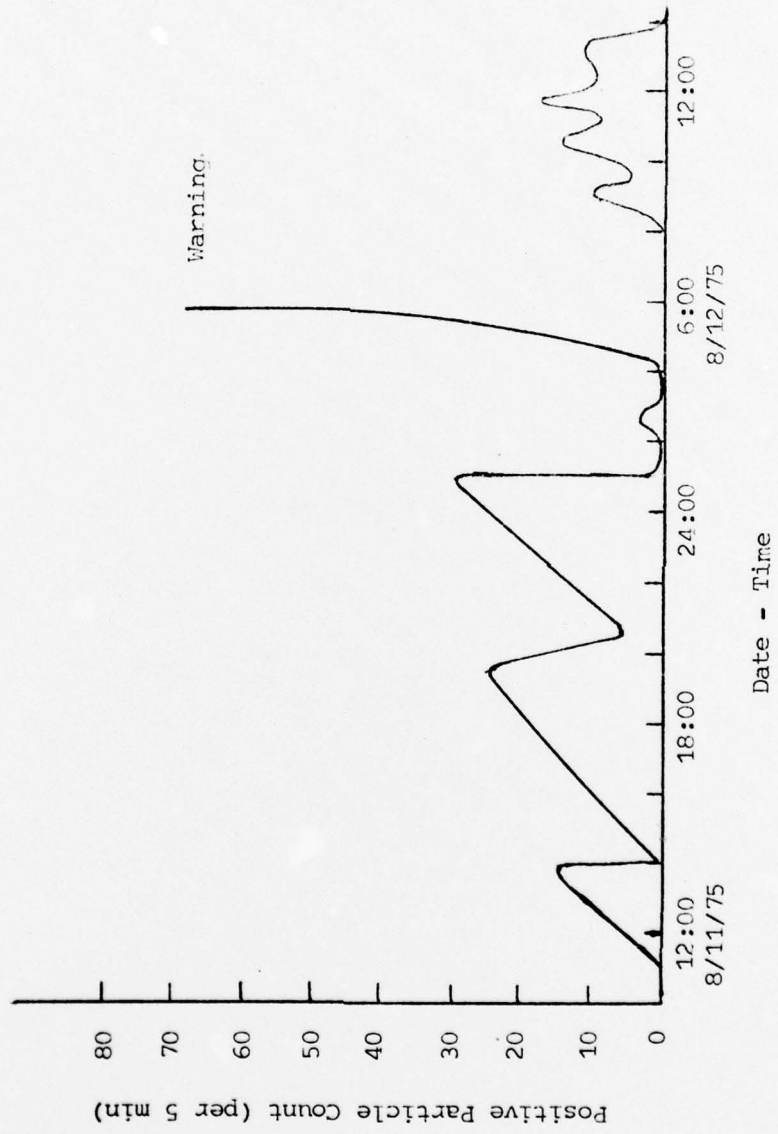


Fig. C-5. TF-41 S/N 141050 (B.U. 52) Particle Count vs Time

Electrostatic Probe Test
 Particle count vs time
 TF41-A-2 engine
 S/N 141050, BU 17
 1000-hr SFE test
 Blue box S/N 4 (trigger level = 500 mv)
 TF41-A-2 probe S/N 1

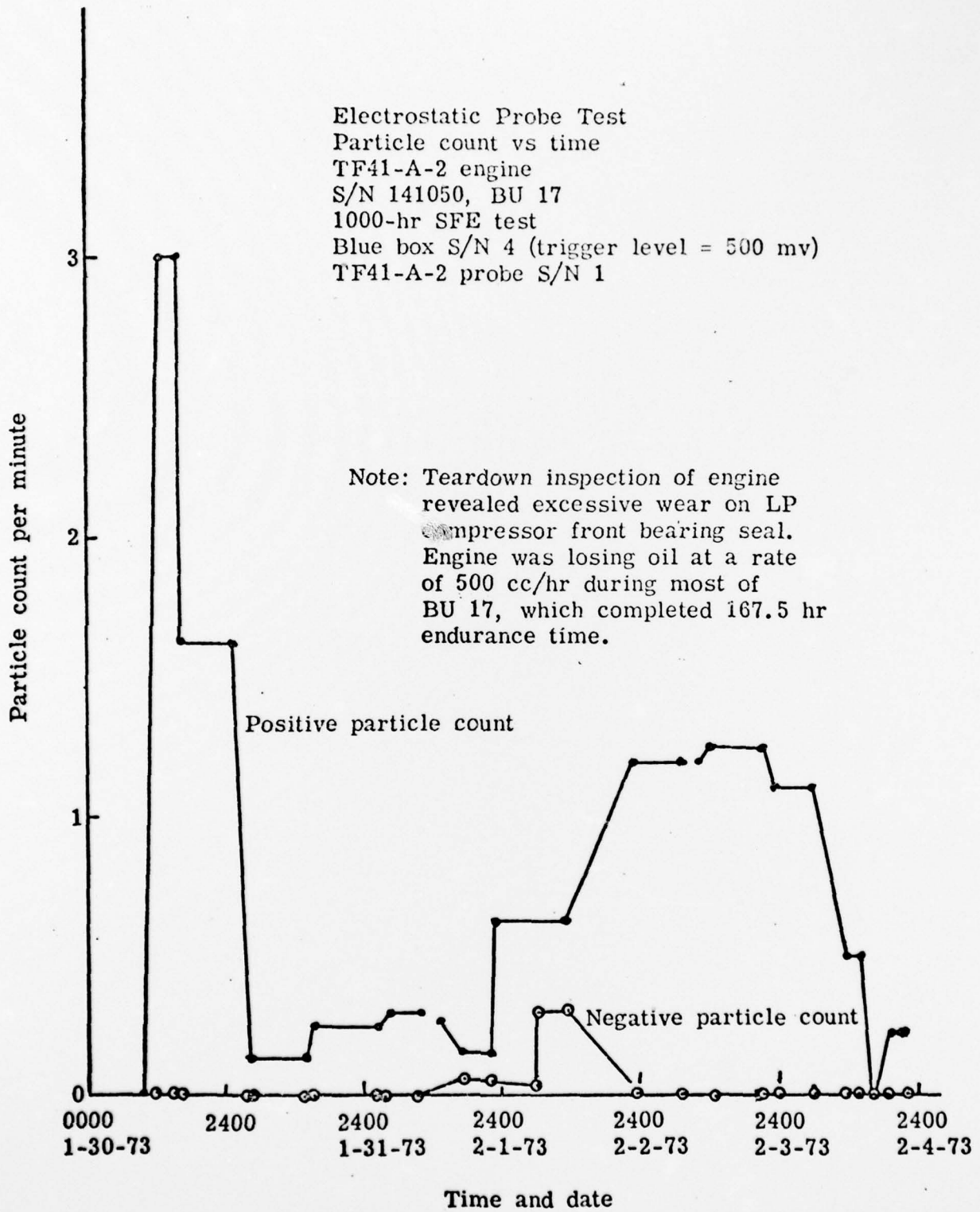


Fig. C-6. TF-41 S/N 141050 (B.U. 17) Particle Count vs Time (Ref 6:62)

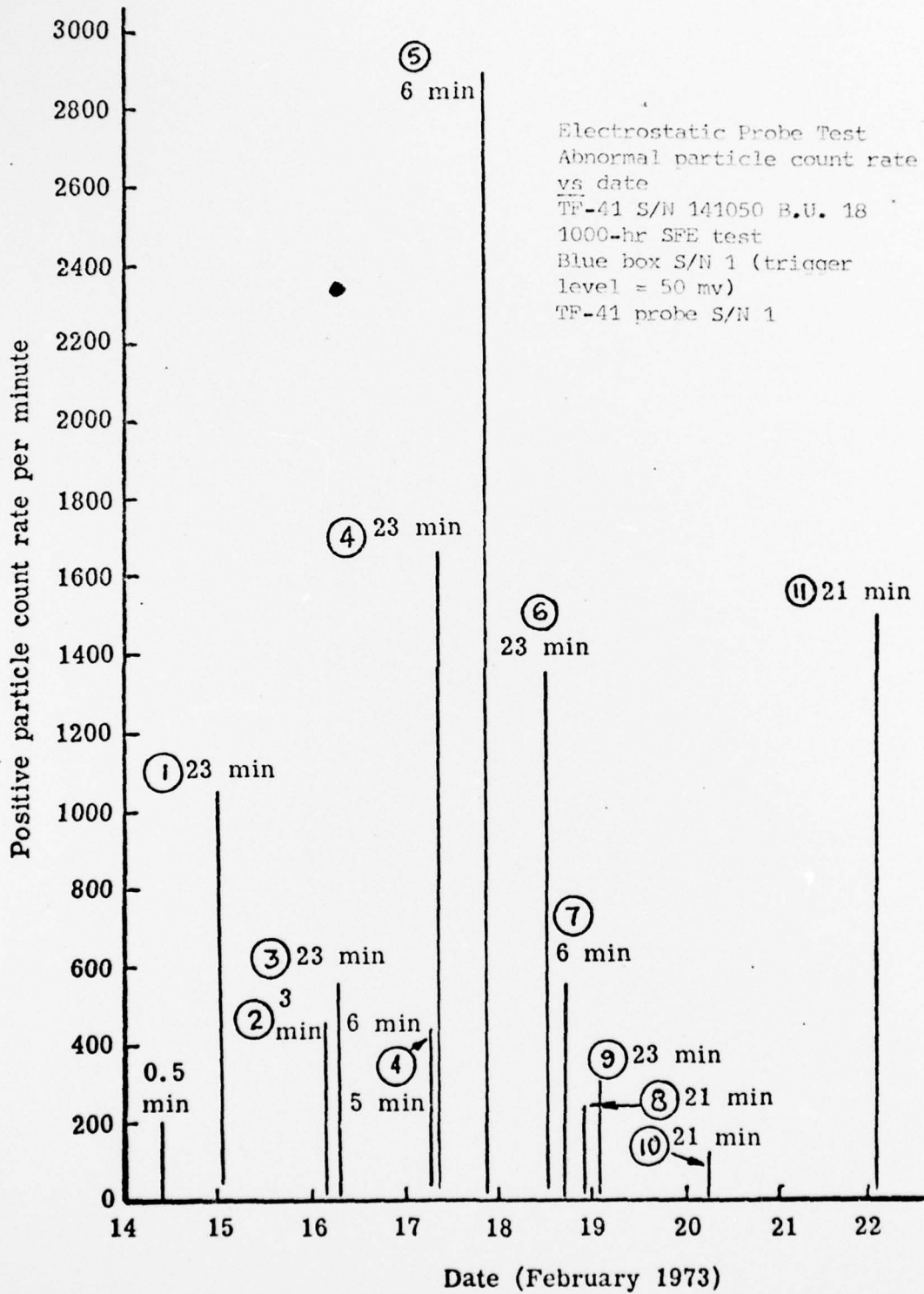


Fig. C-7. TF-41 S/N 141050 (B.U. 18) Peak Particle Count vs Time (First 308 Hrs. of B.U. 18) (Ref 6:64)

Appendix D

Bolus Count History for

TF-41 S/N 908

The following table lists the number of boluses detected by the 2:30 and 6:30 probes during the period in which the non-catastrophic failure of the LP2 turbine occurred. The counts were obtained by using the counting system at Allison Division. Since this system operated independently of the tape recorder, bolus counts were also taken for those cycles which were not recorded. Those cycles which were taped are marked with an asterisk. The cycles are in chronological order.

Although there were B and C cycles interspersed with the A cycles, they have been deleted from the table since they were little interest.

The large number of negative counts on certain cycles such as A204 or A223 do not indicate negative boluses. Rather they indicate extremely long saturation pulses which disrupted the electronics of the counting system.

Table I

TF-41 S/N 908 Bolus Counts

Date	A Cycle	2:30+	2:30-	6:30+	6:30-	
24 Jun	167*	296	4	162	1	
	168*	369	4	218	3	
	169*	265	2	183	2	
	181*	312	21	209	3	
	182*	215	3	155	0	
	183*	190	2	110	0	
	184	104	0	93	0	
	185	176	1	132	1	
	190*	221	2	123	4	
	191	251	4	113	0	
	192	312	6	126	0	
	193	262	3	131	2	
	194	240	0	125	1	
	195*	225	0	127	1	
	196*	227	0	114	1	
	197*	217	1	95	0	
	198*	238	1	124	1	
	25 Jun	199*	100	0	60	0
		200	115	1	59	0
179		117	1	60	0	
186						
187		438	121	302	108	
188		574	109	380	123	
189		699	179	390	124	
201		405	5	234	4	
202		413	52	222	9	
203*		662	158	349	124	
204*		269	471	406	127	
205*		247	9	180	17	
206		297	1	189	4	
207		336	1	182	4	
26 Jun	208	412	7	283	7	
	209	479	88	351	112	
	221	330	6	248	9	
	222	480	59	480	134	
	223	1226	542	645	219	
	224	530	151	517	149	
	225	527	114	452	128	
	227	504	96	384	83	
	228	316	17	362	28	
	229	326	2	262	3	
210	236	2	139	2		
211	195	3	128	0		

Date	A Cycle	2:30+	2:30-	6:30+	6:30-
26 Jun	212	226	1	153	2
	213	172	1	153	0
	214	160	3	116	0
	215	136	1	127	1
	216	161	2	117	1
	217	160	0	124	1
	218	196	1	133	2
	219	60	0	86	0
	220	134	0	72	0
	180	373	9	193	3
28 Jun	230	266	1	111	3
	231	239	1	160	4
	232	201	4	112	3
	233	263	1	136	1
	241	358	40	265	12
	242	403	13	251	2
	243	405	57	287	15
	244	840	288	295	83
	245	356	46	340	81
	246*				
	247*				
	248*	292	3	201	1
	249*	294	15	206	8
	250*	246	2	153	0
	251*	194	2	161	0
	252			155	2
	253			160	11
	254*			183	2
	255*			173	2
	256*			131	0
	257*			112	1
	258*			106	2
	234*				
29 Jun	235*				
	261*			329	25
	262*			334	106
	263*			623	228
	264*			279	20
	265*			284	6
	266*			292	3
	267			247	6
	268			278	4
	269*			239	1
	270*			104	1
	271*			119	1
	272*			130	1
	273*			131	1
274*			112	0	
235					
236					
237					

↑
2:30 Probe
disconnected
↓

Date	A Cycle	2:30+	2:30-	6:30+	6:30-
29 Jun	238		2:30 Probe		
	239*		disconnected		
	240*				
	259*				
30 Jun	260*				
	281*			260	10
	282*			282	26
	283*			335	31
	284*			345	31
	285*			417	95
	286*			233	6
	287			310	6
	277	6	0	102	1
	278	13	0	245	3
1 Jul	289	289	0	362	37
	279	5	1	72	0
	280	4	0	72	1
	301				
	302	41	0	277	6
	303	21	2	311	3
	304	17	0	177	1
	305	6	1	220	1

VITA

William Edward Gifford III was born on 1 December 1946 in Bangor, Maine. He graduated from high school in Wiesbaden, Germany in 1964 and attended Saint Louis University from which he received the degree of Bachelor of Science in Physics in June 1968. Upon graduation he received a commission in the USAF through the AFROTC program. After completing pilot training, he served as a C-123K pilot in the 311th Tactical Airlift Squadron, Phan Rang AB, Republic of Vietnam. He then served as a KC-135 pilot and flight instructor in the 913th Air Refueling Squadron, Barksdale AFB, Louisiana until entering the School of Engineering, Air Force Institute of Technology, in June 1975.

Permanent address: c/o Col. W. E. Gifford, Jr.
424 Lotus Court
Redlands, California 92373

UNCLASSIFIED

SECURITY CLASSIFICATION OF THIS PAGE (When Data Entered)

REPORT DOCUMENTATION PAGE		READ INSTRUCTIONS BEFORE COMPLETING FORM
1. REPORT NUMBER GNE/PH/76-3 ✓	2. GOVT ACCESSION NO.	3. RECIPIENT'S CATALOG NUMBER
4. TITLE (and Subtitle) A METHOD FOR ANALYSIS OF ELECTROSTATIC PROBE SIGNALS RELATING TO JET-ENGINE MICRODISTRESSES		5. TYPE OF REPORT & PERIOD COVERED MS Thesis
		6. PERFORMING ORG. REPORT NUMBER
7. AUTHOR(s) William E. Gifford III		8. CONTRACT OR GRANT NUMBER(s) F33657-76-C-0055 <i>New</i>
9. PERFORMING ORGANIZATION NAME AND ADDRESS Air Force Institute of Technology (AFIT-EN) Wright-Patterson AFB, Ohio 45433		10. PROGRAM ELEMENT, PROJECT, TASK AREA & WORK UNIT NUMBERS
11. CONTROLLING OFFICE NAME AND ADDRESS ASD/YZS41 Wright-Patterson AFB, Ohio 45433		12. REPORT DATE December 1976
		13. NUMBER OF PAGES 61
14. MONITORING AGENCY NAME & ADDRESS (if different from Controlling Office)		15. SECURITY CLASS. (of this report) Unclassified
		15a. DECLASSIFICATION/DOWNGRADING SCHEDULE
16. DISTRIBUTION STATEMENT (of this Report) Approved for public release; distribution unlimited		
17. DISTRIBUTION STATEMENT (of the abstract entered in Block 20, if different from Report)		
18. SUPPLEMENTARY NOTES Approved for public release; IAW AFR 190-17 <i>J. F. Guess</i> JERRAL F. GUESS, Captain, USAF Director of Information		
19. KEY WORDS (Continue on reverse side if necessary and identify by block number) Ion Probe Electrostatic Probe Jet-Engine Failure Prediction		
20. ABSTRACT (Continue on reverse side if necessary and identify by block number) Various methods of data reduction to correlate electrostatic probe signals with engine gas-path distress were developed and tested. These methods consisted of counting pulse signals, monitoring turbine and compressor vibrations, examining individual pulses to determine significant characteristics, and using the integrated areas of all pulses in a given test cycle to determine the level of engine distress. The systems developed were tested using tape recorded data from a TF-41 undergoing a simulated flight endurance test at Detroit Diesel Allison		

DD FORM 1473

1 JAN 73

EDITION OF 1 NOV 65 IS OBSOLETE

UNCLASSIFIED

SECURITY CLASSIFICATION OF THIS PAGE (When Data Entered) *over*

UNCLASSIFIED

SECURITY CLASSIFICATION OF THIS PAGE(When Data Entered)

20 continued

Division in Indianapolis, Indiana. During the test, the LP2 turbine experienced a non-catastrophic failure due to a seal rub. Tapes recorded during the test indicate that the failure occurred over an 80 hour period in which large (350 msec long, 8 volts high) pulses were observed on accelerations. The vibration signature of the engine also changed during this period. A system which integrated the areas under the pulses showed a factor of 20 increase during the period of highest recorded distress.

UNCLASSIFIED

SECURITY CLASSIFICATION OF THIS PAGE(When Data Entered)